

Clinical Nutrition

The APOA1BP-SREBF-NOTCH axis is associated with reduced atherosclerosis risk in morbidly obese patients --Manuscript Draft--

Manuscript Number:	YCLNU-D-19-01600R1
Article Type:	Full Length Article
Keywords:	Apolipoprotein A1 binding protein, APOA1BP, NOTCH, SREBF, atherosclerosis, inflammation, haematopoiesis, liver.
Corresponding Author:	José Manuel Fernández-Real Hospital Dr. Josep Trueta Girona, Girona SPAIN
First Author:	Jordi Mayneris-Perxachs
Order of Authors:	Jordi Mayneris-Perxachs Josep Puig Rémy Burcelin Marc-Emmanuel Dumas Richard H. Barton Lesley Hoyles José Manuel Fernández-Real Massimo Federici
Abstract:	<p>Background & Aims: Atherosclerosis is characterized by an inflammatory disease linked to excessive lipid accumulation in the artery wall. The Notch signalling pathway has been shown to play a key regulatory role in the regulation of inflammation. Recently, <i>in vitro</i> and pre-clinical studies have shown that apolipoprotein A-I binding protein (AIBP) regulates cholesterol metabolism (SREBP) and NOTCH signalling (haematopoiesis) and may be protective against atherosclerosis, but the evidence in humans is scarce.</p> <p>Methods: We evaluated the APOA1BP-SREBF-NOTCH axis in association with atherosclerosis in two well-characterized cohorts of morbidly obese patients ($n = 78$) within the FLORINASH study, including liver transcriptomics, $^1\text{H-NMR}$ plasma metabolomics, high-resolution ultrasonography evaluating carotid intima-media thickness (cIMT), and haematological parameters.</p> <p>Results: The liver expression levels of APOA1BP were associated with lower cIMT and leukocyte counts, a better plasma lipid profile and higher circulating levels of metabolites associated with lower risk of atherosclerosis (glycine, histidine and asparagine). Conversely, liver SREBF and NOTCH mRNAs were positively associated with atherosclerosis, liver steatosis, an unfavourable lipid profile, higher leukocytes and increased levels of metabolites linked to inflammation and CVD such as branched-chain amino acids and glycoproteins. APOA1BP and NOTCH signalling also had a strong association, as revealed by the negative correlations among APOA1BP expression levels and those of all NOTCH receptors and jagged ligands.</p> <p>Conclusions: We here provide the first evidence in human liver of the putative APOA1BP - SREBF-NOTCH axis signalling pathway and its association with atherosclerosis and inflammation.</p>

1 **The *APOA1BP-SREBF-NOTCH* axis is associated with**
2 **reduced atherosclerosis risk in morbidly obese patients**

3
4
5
6 Jordi Mayneris-Perxachs^{1,2}, Josep Puig¹, Rémy Burcelin^{3,4}, Marc-
7 Emmanuel Dumas^{5,6}, Richard H. Barton⁵, Lesley Hoyles⁷, Massimo
8 Federici⁸, José-Manuel Fernández-Real^{1,2*}

9
10
11
12 ¹Department of Endocrinology, Diabetes and Nutrition, Hospital of Girona “Dr Josep Trueta”, Departament
13 de Ciències Mèdiques, University of Girona, Girona Biomedical Research Institute (IdibGi), Girona, Spain

14 ² CIBERObn Pathophysiology of Obesity and Nutrition, Instituto de Salud Carlos III, Madrid, Spain

15 ³ Institut National de la Santé et de la Recherche Médicale (INSERM), Toulouse, France

16 ⁴ Université Paul Sabatier (UPS), Unité Mixte de Recherche (UMR) 1048, Institut des Maladies
17 Métaboliques et Cardiovasculaires (I2MC), Team 2: 'Intestinal Risk Factors, Diabetes, Dyslipidemia, and
18 Heart Failure' F-31432 Toulouse Cedex 4, France

19 ⁵ Section of Computational and Systems Medicine, Division of Integrative Systems Medicine, Department
20 of Metabolism, Digestion and Reproduction, Imperial College London, Exhibition Road, London SW7
21 2AZ, United Kingdom

22 ⁶ Section of Genomic and Environmental Medicine, National Heart & Lung Institute, Imperial College
23 London, Dovehouse Street, SW3 6KY London, United Kingdom

24 ⁷ Department of Biosciences, Nottingham Trent University, Clifton Campus, Nottingham NG11 8NS,
25 United Kingdom

26 ⁸Department of Systems Medicine, University of Rome Tor Vergata, Via Montpellier 1 00133, Rome, Italy

27
28 **Corresponding author:**

29 José-Manuel Fernández-Real, M.D., PhD.

30 Department of Diabetes, Endocrinology and Nutrition.

31 Dr. Josep Trueta University Hospital. Girona Biomedical Research Institute (IdIBGi).

32 Carretera de França s/n, 17007, Girona, Spain.

33 Phone: +34 972940200 / Fax: +34 97294027.

34 E-mail: jmfreal@idibgi.org

35
36 **Running title:** *APOA1BP-SREBF-NOTCH* axis and atherosclerosis risk

37
38 **Keywords:** apolipoprotein A1 binding protein, *APOA1BP*, *NOTCH*, *SREBF*,
39 atherosclerosis, inflammation, haematopoiesis, liver

40

41 **Abbreviations**

42 AAV, adeno-associated virus; ABCA1, ATP-binding cassette transporter A1; AIBP,
43 apolipoprotein A-I binding protein; APOA1, apolipoprotein A1; ALT, alanine
44 aminotransferase; AST, aspartate aminotransferase; BCAA, branched-chain amino acids;
45 CCA; common carotid arteries; cIMT, carotid intima-media thickness; CAD, coronary
46 artery disease; HbA1c, glycated haemoglobin; HDL, high-density lipoprotein; HOMA-
47 IR, homeostasis model assessment of insulin resistance; HPSC, hematopoietic progenitor
48 and stem cells; HsCRP, high sensitive C-reactive protein; ICA, internal carotid arteries;
49 LCAT, lecithin-cholesterol acyltransferase; MWAS, metabolite-wide association studies;
50 NAG, N-acetylglycoproteins; O-PLS, orthogonal partial least squares; PCA, principal
51 component analysis; preCCA, pre bifurcation common carotid arteries; proCCA,
52 proximal segment common carotid arteries; RBC, red blood cells; RCT, reverse
53 cholesterol transport; SR-BI; scavenger receptor class B member 1; TG, triglycerides;
54 WBC, white blood cells

55 **Abstract**

56 **Background & Aims:** Atherosclerosis is characterized by an inflammatory disease
57 linked to excessive lipid accumulation in the artery wall. The Notch signalling pathway
58 has been shown to play a key regulatory role in the regulation of inflammation. Recently,
59 *in vitro* and pre-clinical studies have shown that apolipoprotein A-I binding protein
60 (AIBP) regulates cholesterol metabolism (SREBP) and NOTCH signalling
61 (haematopoiesis) and may be protective against atherosclerosis, but the evidence in
62 humans is scarce.

63 **Methods:** We evaluated the *APOA1BP-SREBF-NOTCH* axis in association with
64 atherosclerosis in two well-characterized cohorts of morbidly obese patients ($n = 78$)
65 within the FLORINASH study, including liver transcriptomics, ¹H-NMR plasma
66 metabolomics, high-resolution ultrasonography evaluating carotid intima-media
67 thickness (cIMT), and haematological parameters.

68 **Results:** The liver expression levels of *APOA1BP* were associated with lower cIMT and
69 leukocyte counts, a better plasma lipid profile and higher circulating levels of metabolites
70 associated with lower risk of atherosclerosis (glycine, histidine and asparagine).
71 Conversely, liver *SREBF* and *NOTCH* mRNAs were positively associated with
72 atherosclerosis, liver steatosis, an unfavourable lipid profile, higher leukocytes and
73 increased levels of metabolites linked to inflammation and CVD such as branched-chain
74 amino acids and glycoproteins. *APOA1BP* and NOTCH signalling also had a strong
75 association, as revealed by the negative correlations among *APOA1BP* expression levels
76 and those of all NOTCH receptors and jagged ligands.

77 **Conclusions:** We here provide the first evidence in human liver of the putative
78 *APOA1BP-SREBF-NOTCH* axis signalling pathway and its association with
79 atherosclerosis and inflammation.

80 Atherosclerosis is the major cause of cardiovascular disease (CVD), the leading cause of
81 death worldwide. Several studies have shown the anti-atherogenic potential of the high-
82 density lipoprotein (HDL)-mediated reverse cholesterol transport (RCT) [1]. In this
83 process, excess cholesterol is transported from macrophages and peripheral tissues back
84 to the liver for excretion. A critical part of RCT is cholesterol efflux, in which intracellular
85 cholesterol is released and collected by apolipoprotein A1 (APOA1), the major
86 component of HDL [2]. In fact, the cholesterol efflux potential of HDL is a better
87 predictor of CVD than circulating HDL levels [3]. The ATP-binding cassette transporter
88 A1 (ABCA1), a cell-membrane protein, is the major transporter that mediates this
89 assembly of cholesterol with APOA1, which is the rate-limiting step in the formation of
90 nascent HDLs.

91 The APOA1 binding protein (AIBP), encoded by *APOA1BP* in humans, is a secreted
92 protein physically associated with APOA1 [4] that enhances cholesterol efflux *in vitro*
93 from macrophages [5] and endothelial cells [6] in the presence of APOA1 or HDL, partly
94 by facilitating apoA1 binding to ABCA1 and preventing ABCA1 degradation [5].
95 Recently, AIBP has shown to protect against atherosclerosis *in vivo* in *ApoE*^{-/-} and *Ldlr*^{-/-}
96 mice by promoting cholesterol efflux and ameliorating inflammation [7,8]. Human
97 *APOA1BP* mRNA is ubiquitously expressed and abundant in most human secretory
98 organs, with the highest expression in kidney, heart, liver, thyroid gland, adrenal gland,
99 and testis [4]. It is of note that kidney and liver are the major sites of APOA1 catabolism.

100 Atherosclerosis is characterized by progressive accumulation of lipids and leukocytes in
101 the intima layer of the arterial wall. It is considered a chronic inflammation disease with
102 monocytes/macrophages, the main immune cells of the innate immune response, playing
103 a major role in all stages of atherosclerosis [9]. Notably, the Notch pathway is well-
104 recognized as a major regulator of cell fate in stem cells and the differentiation of the

105 various cell types of the immune system [10]. Recently, the Notch signalling pathway
106 was shown to play an important role in the onset and progression of atherosclerosis by
107 promoting inflammation through induction of a pro-inflammatory M1 phenotype in
108 macrophages, a switch towards a Th-1 like inflammatory phenotype in differentiated
109 regulatory T cells, and promoting CD8 cytotoxic T cells [11].

110 Recent evidence suggests a control of hematopoietic progenitor and stem cells (HPSC)
111 by cholesterol pathways [12], thereby linking haematopoiesis with atherosclerosis.
112 Interestingly, a connection between AIBP-mediated cholesterol metabolism and Notch
113 signalling has been described recently. AIBP was shown to regulate Notch signalling
114 through relocalization of γ -secretase from lipid to non-lipid rafts in mice [13] and
115 zebrafish Aibp2-mediated cholesterol efflux was shown to activate endothelial Srebp2,
116 which in turn trans-activates Notch and promotes HSPC emergence. These observations
117 suggest a role for the AIBP-SREBP-NOTCH axis in atherosclerosis [14]. Although the
118 bone marrow is the primary site of haematopoiesis in adults, the liver is the main site
119 during prenatal development and hepatic haematopoiesis is believed to persist into
120 adulthood [15,16].

121 No study has, to date, addressed the potential association between AIBP and Notch
122 signalling in humans. Here, we studied this connection in two well-characterized cohorts
123 of morbidly obese patients recruited to the FLORINASH study (17) combining hepatic
124 transcriptome, plasma metabolome, and carotid intima-media thickness (cIMT)
125 measures.

126

127 **Subjects and Methods**

128 **STUDY POPULATION AND SAMPLE COLLECTION**

129 The study population ($n = 78$) included two cohorts of morbidly obese patients aged 22
130 to 61 years old recruited at the Endocrinology Service of the Hospital Universitari de
131 Girona Dr Josep Trueta (Girona, Spain, $n = 32$) and at the Center for Atherosclerosis of
132 Policlinico Tor Vergata University of Rome (Rome, Italy, $n = 46$), as part of the
133 FLORINASH study [17]. All subjects gave written informed consent, which was
134 validated and approved by the ethical committees of the Hospital Universitari Dr Josep
135 Trueta (Comitè d'Ètica d'Investigació Clínica, approval number 2009 046) and
136 Policlinico Tor Vergata University of Rome (Comitato Etico Indipendente, approval
137 number 28-05-2009). Inclusion criteria included Caucasian origin, stable body weight 3
138 months before the study, free of any infection one month preceding the study and absence
139 of any systemic disease. Exclusion criteria included presence of liver disease and thyroid
140 dysfunction, alcohol consumption (> 20 g/day), hepatitis B, drug-induced liver injury,
141 and dyslipidaemia medication. Plasma samples were obtained during the week before
142 elective gastric bypass surgery, during which a liver biopsy was sampled. All samples
143 were stored at -80 °C. Liver samples were collected in RNAlater, fragmented and
144 immediately flash frozen in liquid nitrogen before storage at -80 °C.

145

146 **ANTHROPOMETRIC AND LABORATORY MEASUREMENTS**

147 Blood pressure was measured using a blood pressure monitor (Hem-703C, Omron,
148 Barcelona, Spain), with the subject seated and after 5 min of rest. Three readings were
149 obtained and the mean value was used in the analyses. Waist circumference was measured
150 with a soft tape midway between the lowest rib and the iliac crest. Obesity was considered
151 as a body mass index (BMI) ≥ 30 kg/m².

152 After 8 h fasting, blood was drawn for the measurement of plasma lipids, glucose and
153 insulin. Glucose and lipids were determined by standard laboratory methods. Intra-assay
154 and inter-assay coefficients of variation (CV) were less than 4 %. Serum insulin was
155 measured in duplicate using a monoclonal immunoradiometric assay (Medgenix
156 Diagnostics, Fleunes, Belgium). The intra-assay CV was 5.2 % at a concentration of 10
157 mU/L and 3.4 % at 130 mU/L. The interassay CVs were 6.9 % and 4.5 % at 14 and 89
158 mU/L, respectively. Glycated haemoglobin (HbA1c) was measured by high-pressure
159 liquid chromatography using a fully automated glycated haemoglobin analyser system
160 (Hitachi L-9100; Hitachi, Tokyo, Japan). Insulin resistance was determined by the
161 homeostasis model assessment of insulin resistance (HOMA-IR). High sensitive C-
162 reactive protein (HsCRP) was determined by ultrasensitive assay (Beckman, Fullerton,
163 CA), with intra-and inter-assay CVs of 4 %. Serum alanine aminotransferase (ALT) and
164 aspartate aminotransferase (AST) levels were determined using enzymatic methods.

165

166 **LIVER HISTOLOGY**

167 Liver biopsies were analysed by a single pathologist expert in hepatic pathology. For each
168 liver sample, haematoxylin and eosin, reticulin, and Masson's trichrome staining were
169 performed. Hepatic steatosis grade was determined according to the scoring system for
170 NAFLD and defined as absent (grade 0: <5% steatosis), mild (grade 1: 5-33% steatosis),
171 moderate (grade 2: >33-66% steatosis) or severe (grade 3: >66% steatosis) [18]. Images
172 were independently evaluated by two radiologists blinded to clinical and laboratory data.

173

174

175 **¹H NUCLEAR MAGNETIC RESONANCE (¹H-NMR) METABOLIC**
176 **PROFILING**

177 Metabolomics analyses have been previously described [17]. Briefly, plasma samples
178 were thawed at room temperature and 350 μ L aliquots were carefully placed in 5-mm
179 NMR tubes. Then, 150 μ L of saline solution (0.9 % NaCl) were added and the mixture
180 was gently vortexed. Spectroscopic analyses were performed on a Bruker DRX600
181 spectrometer equipped with either a 5-mm TXI probe operating at 600.13 MHz or a 5-
182 mm BBI probe operating at 600.44 MHz. Spectra were acquired using a water suppressed
183 Carr-Purcell-Meiboom-Gill using the Bruker program *cpmgpr* (RD $90^\circ-(\tau-180^\circ-\tau)$ n-
184 acquire). A RD of 2 s was employed for net magnetization relaxation, during which noise
185 irradiation was applied in order to suppress the large water proton signal. A number of
186 loops $n = 100$ and a spin-echo delay $\tau = 400 \mu$ s was used to allow spectral editing through
187 T2 relaxation and therefore attenuation of broad signals. For each sample, 128 scans were
188 recorded in 32K data points with a spectral width of 20 ppm. All NMR spectra were
189 processed using Topspin (Bruker Biospin, UK). Free induction decays were multiplied
190 by an exponential function corresponding to a line broadening of 0.3 Hz and Fourier
191 transformed. Spectra were automatically phased, baseline-corrected and referenced to the
192 anomeric doublet of glucose (5.23 ppm). The spectra were all then imported to MATLAB
193 and the region around the water resonance ($\delta=4.5-5.0$) was removed.

194

195 **TRANSCRIPTOMICS**

196 Transcriptomic analyses have been previously described [17]. Briefly, RNA from liver
197 biopsy samples was extracted using standard extraction protocols (TRIzol) by Miltenyi
198 Biotec as previously reported. RNA quality (gel images, RNA integrity number and
199 electropherograms) was assessed using an Agilent 2100 Bioanalyzer platform (Agilent

200 Technologies). An RNA integrity number >6 was considered sufficient for gene
201 expression experiments [19]. One-hundred ng of total RNA were used for linear T7-based
202 amplification of RNA for each sample. cDNA was prepared by amplification of the RNA
203 and labelled with Cy3 using the Agilent Low Input Quick Amp Labeling Kit according
204 to the manufacturer's instructions. The amounts of cDNA and dye that were incorporated
205 were measured by an ND-1000 spectrophotometer (NanoDrop Technologies).
206 Hybridization of the Agilent Whole Human Genome Oligo Microarrays 4 × 44K was
207 done following the Agilent 60-mer oligo microarray processing protocol using the
208 Agilent Gene Expression Hybridization Kit. The fluorescence signals of the hybridized
209 Agilent microarrays were detected using Agilent's Microarray Scanner after washing
210 with Agilent Gene Expression Wash Buffer twice and with acetonitrile once. Feature
211 intensities were determined using Agilent Feature Extraction Software. Microarray data
212 were processed and normalized using R and the BioConductor package LIMMA (Linear
213 Models for Microarray Data) [20]. Raw data quality was assessed using pseudoMA and
214 box plots. A background correction was applied and normalization of the green channel
215 between arrays was done using 'cyclicloess' between pairs of arrays. Control and low-
216 expressed probes were removed and only those probes brighter than the negative controls
217 ($\geq 10\%$) on at least one array were kept. Batch-corrected data were obtained using
218 removeBatchEffect based on 'Batch' [20]. Probes with no associated gene ID were
219 removed. Finally, data were averaged based on an association to a particular gene.

220

221

222 **HIGH-RESOLUTION ULTRASONOGRAPHY CAROTID EVALUATION**

223 Carotid arteries were assessed using a Siemens Acuson S2000 (Mochida Siemens
224 Medical System, Tokyo, Japan) ultrasound system with a 7.5 MHz linear array
225 transducer. Images were independently evaluated by two radiologists blinded to clinical
226 and laboratory data. cIMT values were manually measured in 12 carotid segments:
227 internal (i) and external walls (e) of the right and left common carotid arteries (CCA) in
228 a proximal segment (proCCA), in a plaque-free segment 10 mm from the bifurcation
229 (preCCA) and in the internal carotid arteries (ICA). For the left and right arteries, the
230 mean CCA and ICA values for each subject were calculated from these four
231 measurements (mRCCA and mLCCA) and two measurement (mRICA and mLICA),
232 respectively. The average of all measurements was reported as overall cIMT (mCA). Sub-
233 clinical atherosclerosis was defined as a cut-off value of overall cIMT >0.78 mm [21]. A
234 plaque was defined as a focal thickening ≥ 1.2 mm in any of 12 carotid segments (near
235 and far walls of the right and left common carotid arteries, bifurcation and internal carotid
236 artery).

237

238 **STATISTICAL ANALYSES**

239 *Univariate statistics.* Data distribution and normality of variables were checked visually,
240 and using the Kolmogorov-Smirnov and Shapiro-Wilk tests. Baseline characteristics are
241 presented as means \pm SEM or as median [interquartile range (IQR)] if the distribution
242 was not normal. Baseline differences in laboratory and anthropometric variables were
243 assessed using a *t*-test and a Mann-Whitney U test for normally- and non-normally
244 distributed variables, respectively. Since most variables were found to be skewed, partial
245 Spearman's rank correlation was used to test the relationship between clinical variables
246 and *APOA1BP*, *SREBF* and *NOTCH* mRNAs adjusting for age, sex, BMI and country.

247 Analyses were performed with SPSS software (version 23, IBM SPSS Statistics) and
248 MATLAB R2014a. Levels of statistical significance were set at $P < 0.05$.

249 *Multivariate statistics.* Transcriptomic and metabolomic data multivariate statistics were
250 performed in MATLAB R2014a using in-house scripts. This included principal
251 component analysis (PCA) and orthogonal partial least squares (O-PLS) regression on
252 the mean-centered and unit variance-scaled variables. Unsupervised PCA was first
253 applied to visualize the global variance of the data sets to reveal intrinsic similarities,
254 possible confounders, and to identify strong and moderate outliers based on Hotelling's
255 T^2 and distance to the model, respectively. Then, supervised O-PLS regression models
256 were built to identify transcriptomic or metabolic features associated with the variables
257 of interest. Here, the omics profiles were used as the descriptor matrix (X) to predict the
258 response variable (Y). Significant features were selected based on the O-PLS regression
259 loadings adjusted for multiple testing using the Benjamini-Hochberg procedure for false
260 discovery rate (FDR). A $p\text{FDR} < 0.05$ was used as the reference feature selection
261 criterion. Finally, each individual variable identified from multivariate models was
262 further validated by partial Spearman's correlation adjusting for age, BMI, sex and
263 country. The predictive performance of the model (Q^2Y) was calculated using a leave-
264 one-out cross-validation approach and model validity was established by permutation
265 testing (1000 permutations).

266

267

268 **Results**

269 The baseline characteristics of the study participants are shown in Table 1.

270 **ASSOCIATIONS OF *APOA1BP-SREBF-NOTCH* AXIS WITH** 271 **CARDIOVASCULAR AND HAEMATOLOGICAL PARAMETERS**

272 *APOA1BP* had significant inverse associations with several measures of cIMT, including
273 RICAe, RproCCAi, LpreCCAi, LpreCCAe, mLCCA, mCCA, and mCA thickness
274 (Figure 1a). Conversely, the expression levels of *SREBF1* correlated positively with
275 cIMT measures in all segments of the left carotid artery (proximal, pre-bifurcation,
276 internal) and plaque presence. *SREBF2* expression only correlated positively with
277 RpreCCAe. Among the Notch receptors isoforms, *NOTCH2NL* had the strongest
278 correlations with cIMT measures. In particular, it had strong correlations with all
279 measures of the right internal carotid artery, whereas the expression levels of *NOTCH1*
280 and *NOTCH4* were positively correlated with measures in the left carotid artery. Among
281 these genes, only *SREBF1* had a positive association with the steatosis degree (Figure
282 1b). We also correlated the mean of the 12 CCA segments (mCCA) with the expression
283 of all genes involved in cholesterol metabolism. Notably, *SREBF1* was the only gene that
284 correlated positively with mCCA, whereas *APOA1BP* was amongst those having a
285 stronger negative correlation (Figure 1c). Similar results were obtained when mCA was
286 dichotomized based on a subclinical atherosclerosis cut-off >0.78 mm (Supplementary
287 Figure 1a).

288 Given that atherosclerosis is considered a chronic inflammation disease, we examined the
289 associations of atherosclerosis measures with the plasma levels of *N*-acetylglycoproteins
290 (NAG) measured by NMR. NAG is a novel composite biomarker of systemic
291 inflammation that integrates both protein levels and glycosylation states of several of the

292 most abundant acute phase proteins in serum [22]. As expected, NAG levels correlated
293 positively several cIMT measures (Supplementary Figure 1b). As, atherosclerosis is
294 driven by the progressive accumulation of lipids and leukocytes in the arterial wall, we
295 also analysed the association between the expression of the previous genes and lipid and
296 haematological parameters (Figure 1 and Supplementary Figure 1c). Specifically, the
297 expression of *APOA1BP* correlated negatively with WBC counts (Figure 1d), whereas
298 *SREBF1* and *NOTCH2NL* had a positive correlation with RBC (Figure 1e) and WBC
299 (Figure 1f) counts, respectively. The levels of HDL cholesterol (HDL-C) correlated
300 positively with *APOA1BP* expression (Figure 1g), but negatively with the expression of
301 *SREBF1* (Figure 1h). The later also had a positive correlation with the circulating
302 triglyceride (TG) concentration (Figure 1i). Total WBC counts, and in particular
303 lymphocytes and monocytes, also correlated positively with several atherosclerosis
304 measures (Supplementary Figure 1d).

305 ***APOA1BP* and *SREBF* ASSOCIATIONS WITH CHOLESTEROL AND NOTCH** 306 **PATHWAY GENES**

307 O-PLS models were built to identify genes involved in the Notch signalling ($n=79$ genes;
308 Supplementary Table 1) and cholesterol synthesis pathways ($n=109$ genes;
309 Supplementary Table 2) associated with *APOA1BP*, *SREBF1*, and *SREBF2* expression.
310 In the case of *APOA1BP*, significant O-PLS models with a good predictability were
311 obtained for both Notch pathway- (Figure 1j) and cholesterol pathway-associated genes
312 (Figure 1k). Significant genes identified from multivariate O-PLS regression models were
313 further validated by partial Spearman's correlation adjusting for age, BMI, sex, and
314 country (Figure 1l,m). Remarkably, the expression of all Notch receptors (*NOTCH1*,
315 *NOTCH2*, *NOTCH2NL*, *NOTCH3*, *NOTCH4*) and Jagged ligands (*JAG1*, *JAG2*), but not
316 that of delta-like ligands, was negatively associated with the *APOA1BP* expression

317 (Figure 1l). The expression of *APOA1BP* was also associated with the expression of
318 cholesterol transporters such as *ABCA1* and *SCARB1* (Figure 1m). Significant O-PLS
319 models were also obtained for the associations between *SREBF1* expression and genes
320 from both Notch and cholesterol pathways (Supplementary Figure 2a,b). Notably, after
321 partial Spearman's validation (Supplementary Figure 2c,d), the *SREBF1* expression was
322 positively associated with *NOTCH1* and *ABCA1*, which we had found to be negatively
323 associated with *APOA1BP*. Contrary to *SREBF1* results, we did not obtain a significant
324 O-PLS between the expression of *SREBF2* and Notch pathway genes ($Q^2Y=-0.21$).
325 Finally, an O-PLS regression model between cholesterol synthesis pathway genes and
326 *NOTCH2NL* identified a negative association with *APOA1BP*, whereas *ABCA1* had the
327 strongest positive association (Supplementary Figure 2e,f).

328 **ASSOCIATIONS OF THE *APOA1BP-SREBF-NOTCH* AXIS WITH THE SERUM** 329 **METABOLIC PROFILES**

330 O-PLS regression models were built to identify serum metabolites associated with the
331 expression of *APOA1BP*, *SREBF1*, and *SREBF2*. A significant O-PLS model was
332 obtained for the prediction of *APOA1BP* expression levels from the serum metabolic
333 profile (Figure 2a). Significant identified metabolites (Figure 2b) were further validated
334 by partial Spearman's correlation (Figure 2c). We identified asparagine, glycerol,
335 histidine, glycine, choline and citrate as positively associated with the expression of
336 *APOA1BP*, whereas glyceryl of lipids and very low level cholesterol in VLDL were
337 associated negatively. Metabolites associated positively with *APOA1BP* had negative
338 associations with atherosclerosis measures, particularly LmCCA (Figure 2g-i). We also
339 found a borderline significant negative ($r = -0.22$, $P = 0.051$) association between the
340 expression of *APOA1BP* and the inflammatory marker NAG. Metabolome-wide
341 association studies (MWAS) were also performed for the liver expression of *SREBF1* and

342 *SREBF2* using O-PLS multivariate regressions (Figure 2d,e and Supplementary Figure
343 3a) confirmed by partial Spearman's correlation (Figure 2 f and Supplementary Figure
344 3b). As expected, the expression of both genes was positively associated with several
345 lipids. They also had positive associations with inflammatory markers (NAG), branched-
346 chain amino acids (BCAA) (valine, isoleucine) and related catabolites (α -
347 ketoisovalerate), lactate and proline. Most of these metabolites had positive correlations
348 with cIMT measures. In particular, BCAA had positive associations with RICAe (Figure
349 2j-l), whereas NAG and α -ketoisovalerate had positive associations with mCA ($R=0.27$,
350 $P=0.028$; and $R=0.33$, $P=0.006$, respectively).

351

352 **ASSOCIATIONS OF HAEMATOPOIESIS AND LIPIDS WITH THE SERUM** 353 **METABOLIC PROFILES**

354 O-PLS regression models were also constructed to reveal associations between those
355 haematological and lipid parameters associated with the *APOA1BP-SREBF-NOTCH* axis
356 and the serum metabolome. A significant model with a strong predictive ability (Figure
357 3a) was obtained between the serum metabolic profile and the HDL-C levels. After
358 validation of the multivariate-identified metabolites by partial Spearman correlation,
359 metabolites associated with HDL-C were similar to those linked to *APOA1BP* and
360 *SREBF1* (Figure 3b). Hence, phosphocholine, choline, glycerol, and glycine, which
361 correlated positively with the expression of *APOA1BP*, also had a positive correlation
362 with HDL-C. Conversely, several lipids, inflammation-related metabolites (NAG),
363 BCAA (valine, isoleucine) and lactate, which were positively associated with *SREBF1*,
364 had a negative association with the circulating levels of HDL-C. Notably, the expression
365 of *NOTCH2NL* correlated negatively with the serum choline and phosphocholine levels

366 (Figure 3c,d) but positively with the BCAAs leucine and isoleucine (Figure 3e,f). It also
367 had a trend towards a positive association with NAG ($r = 0.20$, $P = 0.07$). A significant
368 O-PLS regression model was also obtained between the fasting serum TG levels and the
369 serum metabolome (Figure 3g). Patients with higher TG concentrations had higher levels
370 of several lipids, BCAAs and catabolites (isoleucine, α -ketoisovalerate), inflammation-
371 related metabolites (NAG), aspartate, proline, and acetone (Figure 3h). As expected, these
372 results agree with those metabolites positively associated with *SREBF1*. Interestingly,
373 several metabolites negatively associated with TG, including glycine, asparagine,
374 phosphocholine, glycerol, and histidine, were found to be positively associated with the
375 expression of *APOA1BP*. Finally, O-PLS regression models (Figure 3i) confirmed by
376 partial Spearman's correlation (Figure 3j) revealed that serum metabolites positively
377 associated with the leukocyte counts were similar to those associated with the expression
378 of *SREBF1*.

379

380 **Discussion**

381 Atherosclerosis and its progression is caused by lipid accumulation and local
382 inflammation of blood vessels, and is the major underlying cause of CVD. High plasma
383 concentrations of HDL have shown anti-atherogenic potential because HDL carries
384 excess cholesterol away from cells. Importantly, human studies have shown that HDL
385 cholesterol efflux capacity, a metric of HDL function that characterizes a key step in RCT,
386 may be athero-protective [1,3]. Recent *in vitro* and animal studies have shown that AIBP
387 may protect against atherosclerosis [5–8]. Here, we provided evidence for the first time,
388 to our knowledge, in humans of an inverse association between the expression of
389 *APOA1BP* and atherosclerosis measures.

390 *In vitro* studies have demonstrated a role of AIBP in promoting cholesterol efflux from
391 human umbilical vein endothelial cells to HDL and THP-1-derived macrophages, thereby
392 reducing lipid accumulation [5,6]. Mechanistically, AIBP enhances cholesterol efflux and
393 RCT by preventing ABCA1 protein degradation through facilitating its binding to
394 APOA1 on the cell membrane, thereby increasing ABCA1 levels [5]. Growing evidence
395 suggests that ABCA1 protects from atherosclerosis by exporting excess cholesterol from
396 cells to poorly lipidated APOA1, which is essential for the biogenesis of nascent HDL in
397 hepatocytes [23]. Recent animal studies have also highlighted the protection of AIBP
398 against atherosclerosis [7,8]. Hence, *ApoE*^{-/-} mice with established atherosclerosis and
399 treated with recombinant adeno-associated virus (rAAV) to overexpress AIBP showed
400 reduction of atherosclerotic plaque size and inflammation but increased circulating HDL
401 levels and RCT to the liver [8]. In the latter model, AIBP was overexpressed in the aorta
402 and peritoneal macrophages, but mainly in the liver. The striking increase in ABCA1
403 protein levels in the aortas and peritoneal macrophages of AIBP-treated mice suggests
404 again that the effects of AIBP are mediated through ABCA1. In another animal study,
405 *ApoA1bp*^{-/-}*Ldlr*^{-/-} mice fed a high-fat, high-cholesterol diet had exacerbated weight gain,
406 liver steatosis, hyperlipidaemia and atherosclerosis compared to *Ldlr*^{-/-} mice [7]. In
407 addition, AAV-mediated overexpression of AIBP in *Ldlr*^{-/-} mice protected against weight
408 gain, plasma lipid increase and atherosclerosis compared to controls.

409 In agreement with these results, we found negative associations between *APOA1BP*
410 expression levels and measures of cIMT. Conversely, we found a negative association
411 between the expression levels of *APOA1BP* and *ABCA1*. It is possible that in patients
412 with reduced hepatic *APOA1BP* expression, there is a compensatory response in the
413 expression of *ABCA1* to increase cholesterol efflux in the liver. In addition, although
414 treatment with AIBP increased ABCA1 protein levels in macrophages and *ApoE*^{-/-} mice,

415 it did not alter the ABCA1 mRNA expression [5,8]. In fact, ABCA1 protein levels and
416 mRNA expression are usually discordant as ABCA1 protein levels are regulated by a
417 diverse posttranscriptional mechanism [24]. In contrast to ABCA1, which is important
418 for the generation of nascent HDL, scavenger receptor class B member 1 (SR-BI) is a
419 receptor for mature HDL and mediates selective uptake of HDL cholesteryl esters into
420 the liver as the final step in RCT [25]. Consistently, we found a significant association
421 between *APOA1BP* and *SCARB1*, which encodes the SR-BI protein, which was opposite
422 to the *APOA1BP-ABCA1* correlation.

423 In addition to the ABCA1 transporter pathway, the VLDL-APOB secretion pathway has
424 been proposed as the major pathway for the secretion of cholesterol from hepatocytes
425 together with TG into plasma [26]. Interestingly, the VLDL secretion pathway is
426 modulated by SREBP1c [27], encoded by *SREBF1*, which we found strongly positively
427 associated with atherosclerosis. Specifically, *SREBF1* correlated with cIMT measures in
428 all segments of the left carotid artery, which is in agreement the higher vulnerability of
429 the left carotid artery to atherosclerosis [28,29]. Hepatic expression of SREBP1c is also
430 increased in hepatic steatosis [30], which is consistent with our results. A recent study in
431 zebrafish has shown that Aibp2-mediated HPSC expansion through the up-regulation of
432 *Srebf2* (but not *Srebf1*), which predominantly regulates cholesterol synthesis [14].
433 Although we mainly found *SREBF1* associated with cIMT rather than *SREBF2*, it is worth
434 noting that *SREBF1* is transcribed into two variants: SREBP-1c, which solely regulates
435 lipid synthesis, and SREBP-1a, which controls both cholesterol and lipid synthesis. AIBP
436 also seem to modulate Notch signalling in mice and zebrafish [13,14]. In agreement with
437 these results, we found strong associations between the expression of *APOA1BP* and the
438 expression of all Notch signalling receptors and jagged ligands, but not with delta-like
439 ligands. Interestingly, jagged and delta-like ligands have shown opposite effects on

440 angiogenesis and regulation of T cells [31,32]. Consistent with a higher susceptibility of
441 the left carotid artery, we also found that *NOTCH1* and *NOTCH4* were positively
442 associated with left cIMT measures. Despite these associations, it is particularly
443 noticeable that the expression of human-specific gene *NOTCH2NL* had the strongest
444 associations with atherosclerotic measures. Interestingly, among all genes involved in
445 cholesterol metabolism, *NOTCH2NL* had the strongest positive association with *ABCA1*,
446 suggesting again a potential upregulation of *ABCA1* expression to increase cholesterol
447 efflux in patients with cIMT. Little is known about *NOTCH2NL*, but it has recently stood
448 out for its ability to enhance Notch signalling and expand human cortical progenitor cells
449 [33,34]. Consistent with this link between cholesterol metabolism and haematopoiesis,
450 we found significant associations among the expression of *APOA1BP*, *SREBF1* and
451 *NOTCH2NL*, and haematology and lipid parameters.

452 We found that the expression of transcripts *APOA1BP*, *SREBF1*, *SREBF2* and
453 *NOTCH2NL* was associated with several plasma metabolites. *APOA1BP* had positive
454 correlations with three amino acids (asparagine, histidine, glycine), glycerol, choline and
455 citrate. These amino acids were also associated positively with circulating HDL-C levels,
456 but negatively with TG and WBC counts. Glycine, histidine and asparagine were also
457 negatively associated with cIMT measures. Of note, among 35 plasma metabolites
458 quantified in 1049 individuals without coronary artery disease (CAD) and diabetes,
459 histidine was most strongly associated with lower risk for incident CAD, followed by
460 asparagine [35]. Low circulating levels of glycine have also been causally associated with
461 higher incidence of coronary heart disease [36].

462 *APOA1BP* expression also had a positive association with choline. Remarkably, both
463 choline and phosphocholine levels had very strong positive associations with HDL-C but
464 correlated negatively with the expression of *NOTCH2NL*. There is evidence suggesting a

465 connection between choline and HDL metabolism. Hence, phosphatidylcholine is the
466 major phospholipid component of all plasma lipoproteins and the biosynthesis of
467 phosphatidylcholine in the liver is critical for the synthesis and secretion of HDL and
468 VLDL [37]. Interestingly, *APOA1BP* correlated negatively with the expression of liver
469 enzymes involved in the synthesis of phosphatidylcholine from choline and
470 phosphocholine, suggesting an up-regulation of the synthesis of phosphatidylcholine in
471 patients with lower *APOA1BP* to increase assembly and clearance of lipoproteins. Due to
472 the role of lecithin–cholesterol acyltransferase (LCAT) in the formation of HDL and
473 RCT, we also assessed the relation between the expression levels of *APOA1BP* and *LCAT*
474 and found a positive association ($R=0.27$, $P=0.01$). Interestingly, although studies in the
475 general population gave inconsistent results, patients with LCAT deficiency have shown
476 a significant increase in the incidence of CVD [38]. Despite the associations with
477 *APOA1BP* and HDL, neither choline nor phosphocholine had associations with measures
478 of atherosclerosis. Previous studies have shown inconsistent associations between
479 circulating choline and phosphocholine levels and cardiovascular events. Both
480 metabolites were positively associated with the risk of CVD and stroke after 4.8 years of
481 follow-up in participants at high cardiovascular risk within the PREDIMED study, but no
482 associations were found between 1-year changes in these metabolites and the incidence
483 of CVD [39]. Similarly, higher plasma choline levels were associated with increased risk
484 of major cardiac events after 3 years of follow-up in patients undergoing elective
485 diagnostic coronary angiography, but they did not predict risk when trimethylamine *N*-
486 oxide, a choline metabolite, was added to the model [40]. In cross-section studies higher
487 plasma choline concentrations have been associated with an unfavourable
488 cardiometabolic risk factor profile, including lower HDL levels [41,42]. However, it is
489 worth noting that plasma choline levels do not reflect choline status because disturbances

490 in circulating choline arise early in disease development [43,44] and circulating levels
491 may depend on lipid overload. In this sense, plasma choline metabolites differed between
492 normal and overweight men [45]. In addition, both low and high plasma concentrations
493 may be associated with adverse effects [46].

494 As expected, the expression levels of *SREBF1* and *SREBF2* had positive associations with
495 several lipids. These genes also correlated positively with circulating levels of BCAA and
496 catabolites, NAG and lactate. Except for lactate, we found that these metabolites were all
497 positively associated with measure of cIMT. Several cross-section and prospective cohort
498 studies revealed positive associations of BCAA with major metabolic disorders [47] and
499 recently they have also been positively associated with risk factors of CAD, in particular
500 cIMT [48]. Interestingly, we also found a positive correlation between the expression
501 levels of *NOTCH2NL* and BCAA. In line with atherosclerosis being a chronic
502 inflammatory disorder, we found a consistent association between NAG, a novel marker
503 of chronic inflammation [22], and cIMT measures. Consistently, we found that NAG
504 levels were the strongest predictors of WBC counts, which also had positive associations
505 with BCAA. Supporting the role of the *APOA1BP-SREBF-NOTCH* axis and
506 inflammation in atherosclerosis, we also found that NAG levels were negatively
507 associated with the expression of *APOA1BP*, but positively with that of *SREBF1*,
508 *SREBF2*, and *NOTCH2NL*. Finally, most of the metabolites associated with *SREBF1* and
509 *SREBF2* had similar associations with TG, but opposite to those of HDL.

510 The main limitation of our study is its cross-sectional nature. Therefore, we cannot infer
511 cause-effect relationships. Second, the results cannot be extrapolated to the general
512 population, as subjects in the current study were morbidly obese. In addition, we did not
513 measure AIBP protein levels. The strengths of the present work include the use of two
514 independent well-characterized cohorts, which allowed the control for potential

515 confounders, with comprehensive metabolomic, transcriptomic, liver biopsy and cIMT
516 data.

517 In conclusion, our findings demonstrate, for the first time, an atheroprotective association
518 between the expression levels of *APOA1BP* and atherosclerosis in humans. We have also
519 shown a connection between *APOA1BP*, Notch signalling and inflammation with
520 atherosclerosis.

521

522 **Acknowledgments**

523 This work was supported by EU-FP7 FLORINASH (Health-F2-2009-241913) to R.B.,
524 M.F., J.M.F.R. Infrastructure support was provided by the National Institute for Health
525 Research (NIHR) Imperial Biomedical Research Centre (BRC). J.M.-P. is funded by the
526 Instituto de Salud Carlos III (Madrid, Spain) through a Miguel Servet programme
527 (CP18/00009). L.H. was in receipt of an MRC Intermediate Research Fellowship (UK
528 MED-BIO; grant number MR/L01632X/1).

529 **References**

- 530 [1] Khera A V., Cuchel M, de la Llera-Moya M, Rodrigues A, Burke MF, Jafri K, et
531 al. Cholesterol Efflux Capacity, High-Density Lipoprotein Function, and
532 Atherosclerosis. *N Engl J Med* 2011;364:127–35. doi:10.1056/NEJMoa1001689.
- 533 [2] Ohashi R, Mu H, Wang X, Yao Q, Chen C. Reverse cholesterol transport and
534 cholesterol efflux in atherosclerosis. *QJM An Int J Med* 2005;98:845–56.
535 doi:10.1093/qjmed/hci136.
- 536 [3] Rohatgi A, Khera A, Berry JD, Givens EG, Ayers CR, Wedin KE, et al. HDL
537 Cholesterol Efflux Capacity and Incident Cardiovascular Events. *N Engl J Med*
538 2014;371:2383–93. doi:10.1056/NEJMoa1409065.
- 539 [4] Ritter M, Buechler C, Boettcher A, Barlage S, Schmitz-Madry A, Orsó E, et al.
540 Cloning and Characterization of a Novel Apolipoprotein A-I Binding Protein, AI-
541 BP, Secreted by Cells of the Kidney Proximal Tubules in Response to HDL or
542 ApoA-I. *Genomics* 2002;79:693–702. doi:10.1006/geno.2002.6761.
- 543 [5] Zhang M, Li L, Xie W, Wu J-F, Yao F, Tan Y-L, et al. Apolipoprotein A-1
544 binding protein promotes macrophage cholesterol efflux by facilitating
545 apolipoprotein A-1 binding to ABCA1 and preventing ABCA1 degradation.
546 *Atherosclerosis* 2016;248:149–59. doi:10.1016/j.atherosclerosis.2016.03.008.
- 547 [6] Fang L, Choi S-H, Baek JS, Liu C, Almazan F, Ulrich F, et al. Control of
548 angiogenesis by AIBP-mediated cholesterol efflux. *Nature* 2013;498:118–22.
549 doi:10.1038/nature12166.
- 550 [7] Schneider DA, Choi S-H, Agatista-Boyle C, Zhu L, Kim J, Pattison J, et al. AIBP
551 protects against metabolic abnormalities and atherosclerosis. *J Lipid Res*

- 552 2018;59:854–63. doi:10.1194/jlr.M083618.
- 553 [8] Zhang M, Zhao G-J, Yao F, Xia X-D, Gong D, Zhao Z-W, et al. AIBP reduces
554 atherosclerosis by promoting reverse cholesterol transport and ameliorating
555 inflammation in apoE $-/-$ mice. *Atherosclerosis* 2018;273:122–30.
556 doi:10.1016/j.atherosclerosis.2018.03.010.
- 557 [9] Gisterå A, Hansson GK. The immunology of atherosclerosis. *Nat Rev Nephrol*
558 2017;13:368–80. doi:10.1038/nrneph.2017.51.
- 559 [10] Radtke F, MacDonald HR, Tacchini-Cottier F. Regulation of innate and adaptive
560 immunity by Notch. *Nat Rev Immunol* 2013;13:427–37. doi:10.1038/nri3445.
- 561 [11] Vieceli Dalla Sega F, Fortini F, Aquila G, Campo G, Vaccarezza M, Rizzo P.
562 Notch Signaling Regulates Immune Responses in Atherosclerosis. *Front*
563 *Immunol* 2019;10. doi:10.3389/fimmu.2019.01130.
- 564 [12] Soehnlein O, Swirski FK. Hypercholesterolemia links hematopoiesis with
565 atherosclerosis. *Trends Endocrinol Metab* 2013;24:129–36.
566 doi:10.1016/j.tem.2012.10.008.
- 567 [13] Mao R, Meng S, Gu Q, Araujo-Gutierrez R, Kumar S, Yan Q, et al. AIBP Limits
568 Angiogenesis Through γ -Secretase-Mediated Upregulation of Notch Signaling.
569 *Circ Res* 2017;120:1727–39. doi:10.1161/CIRCRESAHA.116.309754.
- 570 [14] Gu Q, Yang X, Lv J, Zhang J, Xia B, Kim J, et al. AIBP-mediated cholesterol
571 efflux instructs hematopoietic stem and progenitor cell fate. *Science* (80-)
572 2019;363:1085–8. doi:10.1126/science.aav1749.
- 573 [15] Muench MO, Beyer AI, Fomin ME, Thakker R, Mulvaney US, Nakamura M, et

574 al. The Adult Livers of Immunodeficient Mice Support Human Hematopoiesis:
575 Evidence for a Hepatic Mast Cell Population that Develops Early in Human
576 Ontogeny. PLoS One 2014;9:e97312. doi:10.1371/journal.pone.0097312.

577 [16] Golden-Mason L, O’Farrelly C. Having it all? Stem cells, haematopoiesis and
578 lymphopoiesis in adult human liver. Immunol Cell Biol 2002;80:45–51.
579 doi:10.1046/j.1440-1711.2002.01066.x.

580 [17] Hoyles L, Fernández-Real J-M, Federici M, Serino M, Abbott J, Charpentier J, et
581 al. Molecular phenomics and metagenomics of hepatic steatosis in non-diabetic
582 obese women. Nat Med 2018;24:1070–80. doi:10.1038/s41591-018-0061-3.

583 [18] Kleiner DE, Brunt EM, Van Natta M, Behling C, Contos MJ, Cummings OW, et
584 al. Design and validation of a histological scoring system for nonalcoholic fatty
585 liver disease. Hepatology 2005;41:1313–21. doi:10.1002/hep.20701.

586 [19] Fleige S, Pfaffl MW. RNA integrity and the effect on the real-time qRT-PCR
587 performance. Mol Aspects Med 2006;27:126–39.
588 doi:10.1016/j.mam.2005.12.003.

589 [20] Smyth GK. limma: Linear Models for Microarray Data. Bioinforma. Comput.
590 Biol. Solut. Using R Bioconductor, New York: Springer-Verlag; 2005, p. 397–
591 420. doi:10.1007/0-387-29362-0_23.

592 [21] Touboul P-J, Hennerici MG, Meairs S, Adams H, Amarenco P, Bornstein N, et
593 al. Mannheim carotid intima-media thickness and plaque consensus (2004-2006-
594 2011). An update on behalf of the advisory board of the 3rd, 4th and 5th
595 watching the risk symposia, at the 13th, 15th and 20th European Stroke
596 Conferences, Mannheim, Germany, 2004, Brussels, Belgium, 2006, and

- 597 Hamburg, Germany, 2011. *Cerebrovasc Dis* 2012;34:290–6.
598 doi:10.1159/000343145.
- 599 [22] Connelly MA, Otvos JD, Shalaurova I, Playford MP, Mehta NN. GlycA, a novel
600 biomarker of systemic inflammation and cardiovascular disease risk. *J Transl*
601 *Med* 2017;15:219. doi:10.1186/s12967-017-1321-6.
- 602 [23] Wang S, Smith JD. ABCA1 and nascent HDL biogenesis. *BioFactors*
603 2014;40:547–54. doi:10.1002/biof.1187.
- 604 [24] Lv Y, Yin K, Fu Y, Zhang D, Chen W, Tang C. Posttranscriptional Regulation of
605 *ATP-Binding Cassette Transporter A1* in Lipid Metabolism. *DNA Cell Biol*
606 2013;32:348–58. doi:10.1089/dna.2012.1940.
- 607 [25] Hoekstra M. SR-BI as target in atherosclerosis and cardiovascular disease - A
608 comprehensive appraisal of the cellular functions of SR-BI in physiology and
609 disease. *Atherosclerosis* 2017;258:153–61.
610 doi:10.1016/j.atherosclerosis.2017.01.034.
- 611 [26] Shelness GS, Sellers JA. Very-low-density lipoprotein assembly and secretion.
612 *Curr Opin Lipidol* 2001;12:151–7.
- 613 [27] Okazaki H, Goldstein JL, Brown MS, Liang G. LXR-SREBP-1c-phospholipid
614 transfer protein axis controls very low density lipoprotein (VLDL) particle size. *J*
615 *Biol Chem* 2010;285:6801–10. doi:10.1074/jbc.M109.079459.
- 616 [28] Selwaness M, Van Den Bouwhuijsen Q, Van Onkelen RS, Hofman A, Franco
617 OH, Van Der Lugt A, et al. Atherosclerotic plaque in the left carotid artery is
618 more vulnerable than in the right. *Stroke* 2014;45:3226–30.
619 doi:10.1161/STROKEAHA.114.005202.

- 620 [29] Chou CL, Wu YJ, Hung CL, Liu CC, Wang S De, Wu TW, et al. Segment-
621 specific prevalence of carotid artery plaque and stenosis in middle-aged adults
622 and elders in Taiwan: A community-based study. *J Formos Med Assoc*
623 2019;118:64–71. doi:10.1016/j.jfma.2018.01.009.
- 624 [30] Ferré P, Foufelle F. Hepatic steatosis: a role for de novo lipogenesis and the
625 transcription factor SREBP-1c. *Diabetes, Obes Metab* 2010;12:83–92.
626 doi:10.1111/j.1463-1326.2010.01275.x.
- 627 [31] Rutz S, Mordmüller B, Sakano S, Scheffold A. Notch ligands Delta-like1, Delta-
628 like4 and Jagged1 differentially regulate activation of peripheral T helper cells.
629 *Eur J Immunol* 2005;35:2443–51. doi:10.1002/eji.200526294.
- 630 [32] Benedito R, Roca C, Sörensen I, Adams S, Gossler A, Fruttiger M, et al. The
631 notch ligands Dll4 and Jagged1 have opposing effects on angiogenesis. *Cell*
632 2009;137:1124–35. doi:10.1016/j.cell.2009.03.025.
- 633 [33] Fiddes IT, Lodewijk GA, Mooring M, Bosworth CM, Ewing AD, Mantalas GL,
634 et al. Human-Specific NOTCH2NL Genes Affect Notch Signaling and Cortical
635 Neurogenesis. *Cell* 2018;173:1356–1369.e22. doi:10.1016/j.cell.2018.03.051.
- 636 [34] Suzuki IK, Gacquer D, Van Heurck R, Kumar D, Wojno M, Bilheu A, et al.
637 Human-Specific NOTCH2NL Genes Expand Cortical Neurogenesis through
638 Delta/Notch Regulation. *Cell* 2018;173:1370–1384.e16.
639 doi:10.1016/j.cell.2018.03.067.
- 640 [35] Ottosson F, Smith E, Melander O, Fernandez C. Altered Asparagine and
641 Glutamate Homeostasis Precede Coronary Artery Disease and Type 2 Diabetes. *J*
642 *Clin Endocrinol Metab* 2018;103:3060–9. doi:10.1210/jc.2018-00546.

- 643 [36] Wittemans LBL, Lotta LA, Oliver-Williams C, Stewart ID, Surendran P,
644 Karthikeyan S, et al. Assessing the causal association of glycine with risk of
645 cardio-metabolic diseases. *Nat Commun* 2019;10:1060. doi:10.1038/s41467-019-
646 08936-1.
- 647 [37] Cole LK, Vance JE, Vance DE. Phosphatidylcholine biosynthesis and lipoprotein
648 metabolism. *Biochim Biophys Acta - Mol Cell Biol Lipids* 2012;1821:754–61.
649 doi:10.1016/j.bbalip.2011.09.009.
- 650 [38] Ossoli A, Simonelli S, Vitali C, Franceschini G, Calabresi L. Role of LCAT in
651 Atherosclerosis. *J Atheroscler Thromb* 2016;23:119–27. doi:10.5551/jat.32854.
- 652 [39] Guasch- Ferré M, Hu FB, Ruiz- Canela M, Bulló M, Toledo E, Wang DD, et al.
653 Plasma Metabolites From Choline Pathway and Risk of Cardiovascular Disease
654 in the PREDIMED (Prevention With Mediterranean Diet) Study. *J Am Heart*
655 *Assoc* 2017;6. doi:10.1161/JAHA.117.006524.
- 656 [40] Wang Z, Tang WHW, Buffa JA, Fu X, Britt EB, Koeth RA, et al. Prognostic
657 value of choline and betaine depends on intestinal microbiota-generated
658 metabolite trimethylamine-N-oxide. *Eur Heart J* 2014;35:904–10.
659 doi:10.1093/eurheartj/ehu002.
- 660 [41] Roe AJ, Zhang S, Bhadelia RA, Johnson EJ, Lichtenstein AH, Rogers GT, et al.
661 Choline and its metabolites are differently associated with cardiometabolic risk
662 factors, history of cardiovascular disease, and MRI-documented cerebrovascular
663 disease in older adults. *Am J Clin Nutr* 2017;105:1283–90.
664 doi:10.3945/ajcn.116.137158.
- 665 [42] Konstantinova S V., Tell GS, Vollset SE, Nygård O, Bleie Ø, Ueland PM.

- 666 Divergent Associations of Plasma Choline and Betaine with Components of
667 Metabolic Syndrome in Middle Age and Elderly Men and Women. *J Nutr*
668 2008;138:914–20. doi:10.1093/jn/138.5.914.
- 669 [43] Fischer LM, daCosta KA, Kwock L, Stewart PW, Lu T-S, Stabler SP, et al. Sex
670 and menopausal status influence human dietary requirements for the nutrient
671 choline. *Am J Clin Nutr* 2007;85:1275–85. doi:10.1093/ajcn/85.5.1275.
- 672 [44] Bae S, Ulrich CM, Neuhauser ML, Malysheva O, Bailey LB, Xiao L, et al.
673 Plasma choline metabolites and colorectal cancer risk in the Women’s Health
674 Initiative Observational Study. *Cancer Res* 2014;74:7442–52. doi:10.1158/0008-
675 5472.CAN-14-1835.
- 676 [45] Yan J, Winter LB, Burns-Whitmore B, Vermeulen F, Caudill MA. Plasma
677 choline metabolites associate with metabolic stress among young overweight
678 men in a genotype-specific manner. *Nutr Diabetes* 2012;2:e49.
679 doi:10.1038/nutd.2012.23.
- 680 [46] Lever M, George PM, Atkinson W, Molyneux SL, Elmslie JL, Slow S, et al.
681 Plasma Lipids and Betaine Are Related in an Acute Coronary Syndrome Cohort.
682 *PLoS One* 2011;6:e21666. doi:10.1371/journal.pone.0021666.
- 683 [47] Zhang Z-Y, Monleon D, Verhamme P, Staessen JA. Branched-Chain Amino
684 Acids as Critical Switches in Health and Disease. *Hypertension* 2018;72:1012–
685 22. doi:10.1161/HYPERTENSIONAHA.118.10919.
- 686 [48] Yang R, Dong J, Zhao H, Li H, Guo H, Wang S, et al. Association of branched-
687 chain amino acids with carotid intima-media thickness and coronary artery
688 disease risk factors. *PLoS One* 2014;9:e99598.

689 doi:10.1371/journal.pone.0099598.

690

691 **Figure Legends**

692 **Figure 1. Associations of expression levels of *APOA1BP*, *SREBFs*, and *NOTCHs* genes**
693 **with cIMT, steatosis, haematology and lipid measures and cholesterol and notch**
694 **pathway genes. a)** Heatmap displaying the partial Spearman's correlation coefficients
695 (adjusted for age, BMI, sex, and cohort) between genes and cIMT measures. * $p < 0.05$,
696 ** $p < 0.01$, *** $p < 0.001$. **b)** Association of expression levels of *SREBF1* with the steatosis
697 degree (ANCOVA and Tukey-kramer tests). **c)** Cholesterol metabolism pathway genes
698 significantly associated with mean CCA based on partial Spearman's correlation adjusted
699 for age, BMI, sex, and cohort. **d-i)** Scatter plots between expression levels of selected
700 genes and haematological and lipid parameters. Partial Spearman's correlation and
701 significance values adjusted for age, BMI, sex, and cohort are shown. **j-k)** Permutation
702 test for the goodness-of-fit (R^2Y) and goodness of prediction (Q^2Y) obtained from the O-
703 PLS models between the expression levels of *APOA1BP* and the expression levels of
704 genes involved in the Notch signalling and cholesterol pathways, respectively. **l-m)**
705 Significant Notch and cholesterol pathway genes associated with *APOA1BP* after further
706 validation of the O-PLS identified genes by partial Spearman's correlation adjusting for
707 age, sex, BMI, and country.

708 **Figure 2. Associations of metabolomics data with the expression levels of *APOA1BP*,**
709 ***SREBF1*, and cIMT measures. a)** Permutation test for the goodness-of-fit (R^2Y) and
710 goodness of prediction (Q^2Y) obtained from the O-PLS models between the expression
711 levels of *APOA1BP* and the serum metabolome. **b)** Significant serum metabolites
712 obtained from the O-PLS model. Statistically significant metabolites are coloured in red
713 if positively associated with *APOA1BP* and blue if negatively associated. **c)** Metabolites
714 associated with *APOA1BP* after further validation of the O-PLS identified metabolites by
715 partial Spearman's correlation adjusting for age, sex, BMI, and country. **d)** Permutation

716 test for the goodness-of-fit (R^2Y) and goodness of prediction (Q^2Y) obtained from the O-
717 PLS models between the expression levels of *SREBF1* and the serum metabolome. **e)**
718 Significant serum metabolites obtained from the O-PLS model. Statistically significant
719 metabolites are coloured in red if positively associated with *SREBF1* and blue if
720 negatively associated. **f)** Metabolites associated with *SREBF1* after further validation of
721 the O-PLS identified metabolites by partial Spearman's correlation adjusting for age, sex,
722 BMI, and country. **g-l)** Scatter plots between selected metabolites and cIMT measures.
723 Partial Spearman's correlation and significance values adjusted for age, BMI, sex, and
724 cohort are shown.

725 **Figure 3. Associations of metabolomics data with the lipid parameters, WBC, and**
726 ***NOTCH2NL* expression levels. a)** Permutation test for the goodness-of-fit (R^2Y) and
727 goodness of prediction (Q^2Y) obtained from the O-PLS models between the expression
728 levels of HDL-C and the serum metabolome. **b)** Metabolites associated with HDL-C after
729 further validation of the O-PLS identified metabolites by partial Spearman's correlation
730 adjusting for age, sex, BMI, and country. **c-f)** Scatter plots between selected metabolites
731 and *NOTCH2NL* expression levels. Partial Spearman's correlation and significance
732 values adjusted for age, BMI, sex, and cohort are shown. **g)** Permutation test for the
733 goodness-of-fit (R^2Y) and goodness of prediction (Q^2Y) obtained from the O-PLS models
734 between the expression levels of TG and the serum metabolome. **h)** Metabolites
735 associated with TG after further validation of the O-PLS identified metabolites by partial
736 Spearman's correlation adjusting for age, sex, BMI, and country. **i)** Permutation test for
737 the goodness-of-fit (R^2Y) and goodness of prediction (Q^2Y) obtained from the O-PLS
738 models between the expression levels of WBC and the serum metabolome. **j)** Metabolites
739 associated with WBC after further validation of the O-PLS identified metabolites by
740 partial Spearman's correlation adjusting for age, sex, BMI, and country.

741 **Supplementary Figure 1. a)** Cholesterol metabolism pathway genes significantly
742 associated with mean CA based on partial Spearman's correlation adjusted for age, BMI,
743 sex, and cohort. **b)** Heatmap displaying the partial Spearman's correlations (adjusted for
744 age, BMI, sex, and cohort) between cIMT measures and inflammation measured by NMR
745 plasma levels of *N*-acetylglycoproteins (NAG). **c)** Heatmap displaying the partial
746 Spearman's correlation coefficients (adjusted for age, BMI, sex, and cohort) between
747 genes and haematological parameters. **d)** Heatmap displaying the partial Spearman's
748 correlation coefficients (adjusted for age, BMI, sex, and cohort) between haematological
749 parameters and cIMT measures.

750 **Supplementary Figure 2. a,b)** Permutation test for the goodness-of-fit (R^2Y) and
751 goodness of prediction (Q^2Y) obtained from the O-PLS models between the expression
752 levels of *SREBF1* and the expression levels of genes involved in Notch signalling and
753 cholesterol synthesis pathways, respectively. **c,d)** Significant Notch signalling and
754 cholesterol pathway genes associated with *SREBF1* after further validation of the O-PLS
755 identified genes by partial Spearman's correlation adjusting for age, sex, BMI, and
756 country, respectively. **e)** Permutation test for the goodness-of-fit (R^2Y) and goodness of
757 prediction (Q^2Y) obtained from the O-PLS models between the expression levels of
758 *NOTCH2NL* and the expression levels of genes involved in cholesterol synthesis
759 pathway. **f)** Significant cholesterol pathway genes associated with *NOTCH2NL* after
760 further validation of the O-PLS identified genes by partial Spearman's correlation
761 adjusting for age, sex, BMI, and country.

762 **Supplementary Figure 3. a)** Permutation test for the goodness-of-fit (R^2Y) and goodness
763 of prediction (Q^2Y) obtained from the O-PLS models between the expression levels of
764 *SREBF2* and the serum metabolome. **b)** Significant serum metabolites obtained from the
765 O-PLS model. Statistically significant metabolites are coloured in red if positively

766 associated with *SREBF2* and blue if negatively associated. **c)** Metabolites associated with
767 *SREBF2* after further validation of the O-PLS identified metabolites by partial
768 Spearman's correlation adjusting for age, sex, BMI, and country

769

Table 1. Baseline characteristics of participants.

Variables	All (n=78)
Age (years)	42.4 ± 1.16
BMI (kg/m ²)	46.2 (42.4-51.1)
Waist circumference (cm)	127.0 (119.5-138.0)
Sex (women, %)	79.2
SBP (mmHg)	134.0 (122.5-144.0)
DBP (mmHg)	81.0 (75.0-90.0)
Biochemistry	
Glucose (mg/dL)	95.0 (88.5-101.5)
HOMA-IR	4.50 (2.95-6.90)
Triglycerides (mg/dL)	112.0 (82.0-143.5)
Total cholesterol (mg/dL)	197.5 ± 4.6
LDL cholesterol (mg/dL)	131.0 ± 4.0
HDL cholesterol (mg/dL)	45.0 (40.0-51.2)
Haematology	
Eosinophils	150.0 (100.0-200.0)
Neutrophils	4810 (3665-5795)
Lymphocytes	2360 ± 86.9
Monocytes	500 (420-600)
Total WBC	7350 (6385-9030)
RBC	4.66 (4.46-4.91)
Liver	
HsCRP	0.88 (0.47-1.39)
AST	19.0 (15.0-28.0)
ALT	30.0 (22.0-43.5)
Steatosis grade (%):	
Grade 0	15.6
Grade 1	33.8
Grade 2	24.7
Grade 3	26.0
Atherosclerosis	
RproCCAi	0.70 (0.60-0.80)
RproCCAe	0.70 (0.60-0.80)
RpreCCAi	0.79 ± 0.03
RpreCCAe	0.72 (0.60-0.80)
RICAi	0.70 (0.60-0.90)
RICAe	0.70 (0.54-0.85)
mRCCA	0.73 ± 0.02
mRICA	0.71 ± 0.02
LproCCAi	0.70 (0.60-0.85)
LproCCAe	0.69 (0.60-0.80)
LpreCCAi	0.80 (0.70-1.0)
LpreCCAe	0.84 ± 0.03
LICAi	0.77 (0.57-0.90)
LICAe	0.70 (0.60-0.87)
mLCCA	0.76 ± 0.02
mLICA	0.73 ± 0.03
mCCA	0.74 ± 0.02
mCA	0.73 ± 0.02

771 Values are expressed as means ± SEM for normally distributed variables and median [IQR] for non-normally
772 distributed variables. ALT, alanine aminotransferase; AST, aspartate aminotransferase; HsCRP, high sensitivity

773 C-reactive protein; e, external; i, internal; ICA, internal carotid artery; L, left; m, mean; preCCA, pre bifurcation
774 common carotid artery; proCCA, proximal segment common carotid artery; R, right; RBC, red blood cells; WBC,
775 white blood cells.

1 **The *APOA1BP-SREBF-NOTCH* axis is associated with**
2 **reduced atherosclerosis risk in morbidly obese patients**

3
4
5
6 Jordi Mayneris-Perxachs^{1,2}, Josep Puig¹, Rémy Burcelin^{3,4}, Marc-
7 Emmanuel Dumas^{5,6}, Richard H. Barton⁵, Lesley Hoyles⁷, Massimo
8 Federici⁸, José-Manuel Fernández-Real^{1,2*}

9
10
11
12 ¹ Department of Endocrinology, Diabetes and Nutrition, Hospital of Girona “Dr Josep Trueta”, Departament
13 de Ciències Mèdiques, University of Girona, Girona Biomedical Research Institute (IdibGi), Girona, Spain

14 ² CIBERobn Pathophysiology of Obesity and Nutrition, Instituto de Salud Carlos III, Madrid, Spain

15 ³ Institut National de la Santé et de la Recherche Médicale (INSERM), Toulouse, France

16 ⁴ Université Paul Sabatier (UPS), Unité Mixte de Recherche (UMR) 1048, Institut des Maladies
17 Métaboliques et Cardiovasculaires (I2MC), Team 2: 'Intestinal Risk Factors, Diabetes, Dyslipidemia, and
18 Heart Failure' F-31432 Toulouse Cedex 4, France

19 ⁵ Section of Computational and Systems Medicine, Division of Integrative Systems Medicine, Department
20 of Metabolism, Digestion and Reproduction, Imperial College London, Exhibition Road, London SW7
21 2AZ, United Kingdom

22 ⁶ Section of Genomic and Environmental Medicine, National Heart & Lung Institute, Imperial College
23 London, Dovehouse Street, SW3 6KY London, United Kingdom

24 ⁷ Department of Biosciences, Nottingham Trent University, Clifton Campus, Nottingham NG11 8NS,
25 United Kingdom

26 ⁸ Department of Systems Medicine, University of Rome Tor Vergata, Via Montpellier 1 00133, Rome, Italy

27
28 **Corresponding author:**

29 José-Manuel Fernández-Real, M.D., PhD.

30 Department of Diabetes, Endocrinology and Nutrition.

31 Dr. Josep Trueta University Hospital. Girona Biomedical Research Institute (IdIBGi).

32 Carretera de França s/n, 17007, Girona, Spain.

33 Phone: +34 972940200 / Fax: +34 97294027.

34 E-mail: jmfreal@idibgi.org

35
36 **Running title:** *APOA1BP-SREBF-NOTCH* axis and atherosclerosis risk

37
38 **Keywords:** apolipoprotein A1 binding protein, *APOA1BP*, *NOTCH*, *SREBF*,
39 atherosclerosis, inflammation, haematopoiesis, liver

40

41 **Abbreviations**

42 AAV, adeno-associated virus; ABCA1, ATP-binding cassette transporter A1; AIBP,
43 apolipoprotein A-I binding protein; APOA1, apolipoprotein A1; ALT, alanine
44 aminotransferase; AST, aspartate aminotransferase; BCAA, branched-chain amino acids;
45 CCA; common carotid arteries; cIMT, carotid intima-media thickness; CAD, coronary
46 artery disease; HbA1c, glycated haemoglobin; HDL, high-density lipoprotein; HOMA-
47 IR, homeostasis model assessment of insulin resistance; HPSC, hematopoietic progenitor
48 and stem cells; HsCRP, high sensitive C-reactive protein; ICA, internal carotid arteries;
49 LCAT, lecithin-cholesterol acyltransferase; MWAS, metabolite-wide association studies;
50 NAG, N-acetylglycoproteins; O-PLS, orthogonal partial least squares; PCA, principal
51 component analysis; preCCA, pre bifurcation common carotid arteries; proCCA,
52 proximal segment common carotid arteries; RBC, red blood cells; RCT, reverse
53 cholesterol transport; SR-BI; scavenger receptor class B member 1; TG, triglycerides;
54 WBC, white blood cells

55 **Abstract**

56 **Background & Aims:** Atherosclerosis is characterized by an inflammatory disease
57 linked to excessive lipid accumulation in the artery wall. The Notch signalling pathway
58 has been shown to play a key regulatory role in the regulation of inflammation. Recently,
59 *in vitro* and pre-clinical studies have shown that apolipoprotein A-I binding protein
60 (AIBP) regulates cholesterol metabolism (SREBP) and NOTCH signalling
61 (haematopoiesis) and may be protective against atherosclerosis, but the evidence in
62 humans is scarce.

63 **Methods:** We evaluated the *APOA1BP-SREBF-NOTCH* axis in association with
64 atherosclerosis in two well-characterized cohorts of morbidly obese patients ($n = 78$)
65 within the FLORINASH study, including liver transcriptomics, ¹H-NMR plasma
66 metabolomics, high-resolution ultrasonography evaluating carotid intima-media
67 thickness (cIMT), and haematological parameters.

68 **Results:** The liver expression levels of *APOA1BP* were associated with lower cIMT and
69 leukocyte counts, a better plasma lipid profile and higher circulating levels of metabolites
70 associated with lower risk of atherosclerosis (glycine, histidine and asparagine).
71 Conversely, liver *SREBF* and *NOTCH* mRNAs were positively associated with
72 atherosclerosis, liver steatosis, an unfavourable lipid profile, higher leukocytes and
73 increased levels of metabolites linked to inflammation and CVD such as branched-chain
74 amino acids and glycoproteins. *APOA1BP* and NOTCH signalling also had a strong
75 association, as revealed by the negative correlations among *APOA1BP* expression levels
76 and those of all NOTCH receptors and jagged ligands.

77 **Conclusions:** We here provide the first evidence in human liver of the putative
78 *APOA1BP-SREBF-NOTCH* axis signalling pathway and its association with
79 atherosclerosis and inflammation.

80 Atherosclerosis is the major cause of cardiovascular disease (CVD), the leading cause of
81 death worldwide. Several studies have shown the anti-atherogenic potential of the high-
82 density lipoprotein (HDL)-mediated reverse cholesterol transport (RCT) [1]. In this
83 process, excess cholesterol is transported from macrophages and peripheral tissues back
84 to the liver for excretion. A critical part of RCT is cholesterol efflux, in which intracellular
85 cholesterol is released and collected by apolipoprotein A1 (APOA1), the major
86 component of HDL [2]. In fact, the cholesterol efflux potential of HDL is a better
87 predictor of CVD than circulating HDL levels [3]. The ATP-binding cassette transporter
88 A1 (ABCA1), a cell-membrane protein, is the major transporter that mediates this
89 assembly of cholesterol with APOA1, which is the rate-limiting step in the formation of
90 nascent HDLs.

91 The APOA1 binding protein (AIBP), encoded by *APOA1BP* in humans, is a secreted
92 protein physically associated with APOA1 [4] that enhances cholesterol efflux *in vitro*
93 from macrophages [5] and endothelial cells [6] in the presence of APOA1 or HDL, partly
94 by facilitating apoA1 binding to ABCA1 and preventing ABCA1 degradation [5].
95 Recently, AIBP has shown to protect against atherosclerosis *in vivo* in *ApoE*^{-/-} and *Ldlr*^{-/-}
96 mice by promoting cholesterol efflux and ameliorating inflammation [7,8]. Human
97 *APOA1BP* mRNA is ubiquitously expressed and abundant in most human secretory
98 organs, with the highest expression in kidney, heart, liver, thyroid gland, adrenal gland,
99 and testis [4]. It is of note that kidney and liver are the major sites of APOA1 catabolism.

100 Atherosclerosis is characterized by progressive accumulation of lipids and leukocytes in
101 the intima layer of the arterial wall. It is considered a chronic inflammation disease with
102 monocytes/macrophages, the main immune cells of the innate immune response, playing
103 a major role in all stages of atherosclerosis [9]. Notably, the Notch pathway is well-
104 recognized as a major regulator of cell fate in stem cells and the differentiation of the

105 various cell types of the immune system [10]. Recently, the Notch signalling pathway
106 was shown to play an important role in the onset and progression of atherosclerosis by
107 promoting inflammation through induction of a pro-inflammatory M1 phenotype in
108 macrophages, a switch towards a Th-1 like inflammatory phenotype in differentiated
109 regulatory T cells, and promoting CD8 cytotoxic T cells [11].

110 Recent evidence suggests a control of hematopoietic progenitor and stem cells (HPSC)
111 by cholesterol pathways [12], thereby linking haematopoiesis with atherosclerosis.
112 Interestingly, a connection between AIBP-mediated cholesterol metabolism and Notch
113 signalling has been described recently. AIBP was shown to regulate Notch signalling
114 through relocalization of γ -secretase from lipid to non-lipid rafts in mice [13] and
115 zebrafish Aibp2-mediated cholesterol efflux was shown to activate endothelial Srebp2,
116 which in turn trans-activates Notch and promotes HSPC emergence. These observations
117 suggest a role for the AIBP-SREBP-NOTCH axis in atherosclerosis [14]. Although the
118 bone marrow is the primary site of haematopoiesis in adults, the liver is the main site
119 during prenatal development and hepatic haematopoiesis is believed to persist into
120 adulthood [15,16].

121 No study has, to date, addressed the potential association between AIBP and Notch
122 signalling in humans. Here, we studied this connection in two well-characterized cohorts
123 of morbidly obese patients recruited to the FLORINASH study (17) combining hepatic
124 transcriptome, plasma metabolome, and carotid intima-media thickness (cIMT)
125 measures.

126

127 **Subjects and Methods**

128 **STUDY POPULATION AND SAMPLE COLLECTION**

129 The study population ($n = 78$) included two cohorts of morbidly obese patients aged 22
130 to 61 years old recruited at the Endocrinology Service of the Hospital Universitari de
131 Girona Dr Josep Trueta (Girona, Spain, $n = 32$) and at the Center for Atherosclerosis of
132 Policlinico Tor Vergata University of Rome (Rome, Italy, $n = 46$), as part of the
133 FLORINASH study [17]. All subjects gave written informed consent, which was
134 validated and approved by the ethical committees of the Hospital Universitari Dr Josep
135 Trueta (Comitè d'Ètica d'Investigació Clínica, approval number 2009 046) and
136 Policlinico Tor Vergata University of Rome (Comitato Etico Indipendente, approval
137 number 28-05-2009). Inclusion criteria included Caucasian origin, stable body weight 3
138 months before the study, free of any infection one month preceding the study and absence
139 of any systemic disease. Exclusion criteria included presence of liver disease and thyroid
140 dysfunction, alcohol consumption (> 20 g/day), hepatitis B, drug-induced liver injury,
141 and dyslipidaemia medication. Plasma samples were obtained during the week before
142 elective gastric bypass surgery, during which a liver biopsy was sampled. All samples
143 were stored at -80 °C. Liver samples were collected in RNAlater, fragmented and
144 immediately flash frozen in liquid nitrogen before storage at -80 °C.

145

146 **ANTHROPOMETRIC AND LABORATORY MEASUREMENTS**

147 Blood pressure was measured using a blood pressure monitor (Hem-703C, Omron,
148 Barcelona, Spain), with the subject seated and after 5 min of rest. Three readings were
149 obtained and the mean value was used in the analyses. Waist circumference was measured
150 with a soft tape midway between the lowest rib and the iliac crest. Obesity was considered
151 as a body mass index (BMI) ≥ 30 kg/m².

152 After 8 h fasting, blood was drawn for the measurement of plasma lipids, glucose and
153 insulin. Glucose and lipids were determined by standard laboratory methods. Intra-assay
154 and inter-assay coefficients of variation (CV) were less than 4 %. Serum insulin was
155 measured in duplicate using a monoclonal immunoradiometric assay (Medgenix
156 Diagnostics, Fleunes, Belgium). The intra-assay CV was 5.2 % at a concentration of 10
157 mU/L and 3.4 % at 130 mU/L. The interassay CVs were 6.9 % and 4.5 % at 14 and 89
158 mU/L, respectively. Glycated haemoglobin (HbA1c) was measured by high-pressure
159 liquid chromatography using a fully automated glycated haemoglobin analyser system
160 (Hitachi L-9100; Hitachi, Tokyo, Japan). Insulin resistance was determined by the
161 homeostasis model assessment of insulin resistance (HOMA-IR). High sensitive C-
162 reactive protein (HsCRP) was determined by ultrasensitive assay (Beckman, Fullerton,
163 CA), with intra- and inter-assay CVs of 4 %. Serum alanine aminotransferase (ALT) and
164 aspartate aminotransferase (AST) levels were determined using enzymatic methods.

165

166 **LIVER HISTOLOGY**

167 Liver biopsies were analysed by a single pathologist expert in hepatic pathology. For each
168 liver sample, haematoxylin and eosin, reticulin, and Masson's trichrome staining were
169 performed. Hepatic steatosis grade was determined according to the scoring system for
170 NAFLD and defined as absent (grade 0: <5% steatosis), mild (grade 1: 5-33% steatosis),
171 moderate (grade 2: >33-66% steatosis) or severe (grade 3: >66% steatosis) [18]. Images
172 were independently evaluated by two radiologists blinded to clinical and laboratory data.

173

174

175 **¹H NUCLEAR MAGNETIC RESONANCE (¹H-NMR) METABOLIC**
176 **PROFILING**

177 Metabolomics analyses have been previously described [17]. Briefly, plasma samples
178 were thawed at room temperature and 350 μ L aliquots were carefully placed in 5-mm
179 NMR tubes. Then, 150 μ L of saline solution (0.9 % NaCl) were added and the mixture
180 was gently vortexed. Spectroscopic analyses were performed on a Bruker DRX600
181 spectrometer equipped with either a 5-mm TXI probe operating at 600.13 MHz or a 5-
182 mm BBI probe operating at 600.44 MHz. Spectra were acquired using a water suppressed
183 Carr-Purcell-Meiboom-Gill using the Bruker program *cpmgpr* (RD 90° -(τ - 180° - τ) n-
184 acquire). A RD of 2 s was employed for net magnetization relaxation, during which noise
185 irradiation was applied in order to suppress the large water proton signal. A number of
186 loops $n = 100$ and a spin-echo delay $\tau = 400 \mu$ s was used to allow spectral editing through
187 T2 relaxation and therefore attenuation of broad signals. For each sample, 128 scans were
188 recorded in 32K data points with a spectral width of 20 ppm. All NMR spectra were
189 processed using Topspin (Bruker Biospin, UK). Free induction decays were multiplied
190 by an exponential function corresponding to a line broadening of 0.3 Hz and Fourier
191 transformed. Spectra were automatically phased, baseline-corrected and referenced to the
192 anomeric doublet of glucose (5.23 ppm). The spectra were all then imported to MATLAB
193 and the region around the water resonance ($\delta=4.5$ -5.0) was removed.

194

195 **TRANSCRIPTOMICS**

196 Transcriptomic analyses have been previously described [17]. Briefly, RNA from liver
197 biopsy samples was extracted using standard extraction protocols (TRIzol) by Miltenyi
198 Biotec as previously reported. RNA quality (gel images, RNA integrity number and
199 electropherograms) was assessed using an Agilent 2100 Bioanalyzer platform (Agilent

200 Technologies). An RNA integrity number >6 was considered sufficient for gene
201 expression experiments [19]. One-hundred ng of total RNA were used for linear T7-based
202 amplification of RNA for each sample. cDNA was prepared by amplification of the RNA
203 and labelled with Cy3 using the Agilent Low Input Quick Amp Labeling Kit according
204 to the manufacturer's instructions. The amounts of cDNA and dye that were incorporated
205 were measured by an ND-1000 spectrophotometer (NanoDrop Technologies).
206 Hybridization of the Agilent Whole Human Genome Oligo Microarrays $4 \times 44K$ was
207 done following the Agilent 60-mer oligo microarray processing protocol using the
208 Agilent Gene Expression Hybridization Kit. The fluorescence signals of the hybridized
209 Agilent microarrays were detected using Agilent's Microarray Scanner after washing
210 with Agilent Gene Expression Wash Buffer twice and with acetonitrile once. Feature
211 intensities were determined using Agilent Feature Extraction Software. Microarray data
212 were processed and normalized using R and the BioConductor package LIMMA (Linear
213 Models for Microarray Data) [20]. Raw data quality was assessed using pseudoMA and
214 box plots. A background correction was applied and normalization of the green channel
215 between arrays was done using 'cyclicloess' between pairs of arrays. Control and low-
216 expressed probes were removed and only those probes brighter than the negative controls
217 ($\geq 10\%$) on at least one array were kept. Batch-corrected data were obtained using
218 removeBatchEffect based on 'Batch' [20]. Probes with no associated gene ID were
219 removed. Finally, data were averaged based on an association to a particular gene.

220

221

222 **HIGH-RESOLUTION ULTRASONOGRAPHY CAROTID EVALUATION**

223 Carotid arteries were assessed using a Siemens Acuson S2000 (Mochida Siemens
224 Medical System, Tokyo, Japan) ultrasound system with a 7.5 MHz linear array
225 transducer. Images were independently evaluated by two radiologists blinded to clinical
226 and laboratory data. cIMT values were manually measured in 12 carotid segments:
227 internal (i) and external walls (e) of the right and left common carotid arteries (CCA) in
228 a proximal segment (proCCA), in a plaque-free segment 10 mm from the bifurcation
229 (preCCA) and in the internal carotid arteries (ICA). For the left and right arteries, the
230 mean CCA and ICA values for each subject were calculated from these four
231 measurements (mRCCA and mLCCA) and two measurement (mRICA and mLICA),
232 respectively. The average of all measurements was reported as overall cIMT (mCA). Sub-
233 clinical atherosclerosis was defined as a cut-off value of overall cIMT >0.78 mm [21]. A
234 plaque was defined as a focal thickening ≥ 1.2 mm in any of 12 carotid segments (near
235 and far walls of the right and left common carotid arteries, bifurcation and internal carotid
236 artery).

237

238 **STATISTICAL ANALYSES**

239 *Univariate statistics.* Data distribution and normality of variables were checked visually,
240 and using the Kolmogorov-Smirnov and Shapiro-Wilk tests. Baseline characteristics are
241 presented as means \pm SEM or as median [interquartile range (IQR)] if the distribution
242 was not normal. Baseline differences in laboratory and anthropometric variables were
243 assessed using a *t*-test and a Mann-Whitney U test for normally- and non-normally
244 distributed variables, respectively. Since most variables were found to be skewed, partial
245 Spearman's rank correlation was used to test the relationship between clinical variables
246 and *APOA1BP*, *SREBF* and *NOTCH* mRNAs adjusting for age, sex, BMI and country.

247 Analyses were performed with SPSS software (version 23, IBM SPSS Statistics) and
248 MATLAB R2014a. Levels of statistical significance were set at $P < 0.05$.

249 *Multivariate statistics.* Transcriptomic and metabolomic data multivariate statistics were
250 performed in MATLAB R2014a using in-house scripts. This included principal
251 component analysis (PCA) and orthogonal partial least squares (O-PLS) regression on
252 the mean-centered and unit variance-scaled variables. Unsupervised PCA was first
253 applied to visualize the global variance of the data sets to reveal intrinsic similarities,
254 possible confounders, and to identify strong and moderate outliers based on Hotelling's
255 T^2 and distance to the model, respectively. Then, supervised O-PLS regression models
256 were built to identify transcriptomic or metabolic features associated with the variables
257 of interest. Here, the omics profiles were used as the descriptor matrix (X) to predict the
258 response variable (Y). Significant features were selected based on the O-PLS regression
259 loadings adjusted for multiple testing using the Benjamini-Hochberg procedure for false
260 discovery rate (FDR). A $p\text{FDR} < 0.05$ was used as the reference feature selection
261 criterion. Finally, each individual variable identified from multivariate models was
262 further validated by partial Spearman's correlation adjusting for age, BMI, sex and
263 country. The predictive performance of the model (Q^2Y) was calculated using a leave-
264 one-out cross-validation approach and model validity was established by permutation
265 testing (1000 permutations).

266

267

268 **Results**

269 The baseline characteristics of the study participants are shown in Table 1.

270 **ASSOCIATIONS OF *APOA1BP-SREBF-NOTCH* AXIS WITH**
271 **CARDIOVASCULAR AND HAEMATOLOGICAL PARAMETERS**

272 *APOA1BP* had significant inverse associations with several measures of cIMT, including
273 RICAe, ~~RpreCCAe~~RpreCCAi, LpreCCAi, LpreCCAe, mLCCA, mCCA, and mCA
274 thickness (Figure 1a). Conversely, the expression levels of *SREBF1* correlated positively
275 with cIMT measures in all segments of the left carotid artery (proximal, pre-bifurcation,
276 internal) and plaque presence. *SREBF2* expression only correlated positively with
277 RpreCCAe. Among the Notch receptors isoforms, *NOTCH2NL* had the strongest
278 correlations with cIMT measures. In particular, it had strong correlations with all
279 measures of the right internal carotid artery, whereas the expression levels of *NOTCH1*
280 and *NOTCH4* were positively correlated with measures in the left carotid artery. Among
281 these genes, only *SREBF1* had a positive association with the steatosis degree (Figure
282 1b). We also correlated the mean of the 12 CCA segments (mCCA) with the expression
283 of all genes involved in cholesterol metabolism. Notably, *SREBF1* was the only gene that
284 correlated positively with mCCA, whereas *APOA1BP* was amongst those having a
285 stronger negative correlation (Figure 1c). Similar results were obtained when mCA was
286 dichotomized based on a subclinical atherosclerosis cut-off >0.78 mm (Supplementary
287 Figure 1a).

288 Given that atherosclerosis is considered a chronic inflammation disease, we examined the
289 associations of atherosclerosis measures with the plasma levels of *N*-acetylglycoproteins
290 (NAG) measured by NMR. NAG is a novel composite biomarker of systemic
291 inflammation that integrates both protein levels and glycosylation states of several of the

292 most abundant acute phase proteins in serum [22]. As expected, NAG levels correlated
293 positively several cIMT measures (Supplementary Figure 1b). As, Atherosclerosis is
294 characterized-driven by the progressive accumulation of lipids and leukocytes in the
295 arterial wall. ~~Therefore,~~ we also analysed the association between the expression of the
296 previous genes and lipid and haematological parameters (Figure 1 and Supplementary
297 Figure 1c). Specifically, the expression of *APOA1BP* correlated negatively with WBC
298 counts (Figure 1d), whereas *SREBF1* and *NOTCH2NL* had a positive correlation with
299 RBC (Figure 1e) and WBC (Figure 1f) counts, respectively. The levels of HDL
300 cholesterol (HDL-C) correlated positively with *APOA1BP* expression (Figure 1g), but
301 negatively with the expression of *SREBF1* (Figure 1h). The later also had a positive
302 correlation with the circulating triglyceride (TG) concentration (Figure 1i). Total WBC
303 counts, and in particular lymphocytes and monocytes, also correlated positively with
304 several atherosclerosis measures (Supplementary Figure 1d).

305 ***APOA1BP* and *SREBF* ASSOCIATIONS WITH CHOLESTEROL AND NOTCH**

306 **PATHWAY GENES**

307 O-PLS models were built to identify genes involved in the Notch signalling (n=79 genes;
308 Supplementary Table 1) and cholesterol synthesis pathways (n=109 genes;
309 Supplementary Table 2) associated with *APOA1BP*, *SREBF1*, and *SREBF2*-expression.
310 In the case of *APOA1BP*, Significant O-PLS models with a good predictability were
311 obtained for both Notch pathway- (Figure 1j) and cholesterol pathway-associated genes
312 (Figure 1k). Significant genes identified from multivariate O-PLS regression models were
313 further validated by partial Spearman's correlation adjusting for age, BMI, sex, and
314 country (Figure 1l,m). Remarkably, the expression of all Notch receptors (*NOTCH1*,
315 *NOTCH2*, *NOTCH2NL*, *NOTCH3*, *NOTCH4*) and Jagged ligands (*JAG1*, *JAG2*), but not
316 that of delta-like ligands, was negatively associated with the *APOA1BP* expression

317 (Figure 1l). The expression of *APOA1BP* was also associated with the expression of
318 cholesterol transporters such as *ABCA1* and *SCARB1* (Figure 1m). Significant O-PLS
319 models were also obtained for the associations between *SREBF1* expression and genes
320 from both Notch and cholesterol pathways (Supplementary Figure 2a,b). Notably, after
321 partial Spearman's validation (Supplementary Figure 2c,d), the *SREBF1* expression was
322 positively associated with *NOTCH1* and *ABCA1*, which we had found to be negatively
323 associated with *APOA1BP*. Contrary to *SREBF1* results, we did not obtain a significant
324 O-PLS between the expression of *SREBF2* and Notch pathway genes ($Q^2Y=-0.21$).
325 Finally, An O-PLS regression model between cholesterol synthesis pathway genes and
326 *NOTCH2NL* identified a negative association with *APOA1BP*, whereas *ABCA1* had the
327 strongest positive association (Supplementary Figure 2e,f).

328 **ASSOCIATIONS OF THE *APOA1BP-SREBF-NOTCH* AXIS WITH THE SERUM** 329 **METABOLIC PROFILES**

330 O-PLS regression models were built to identify serum metabolites associated with the
331 expression of *APOA1BP*, *SREBF1*, and *SREBF2*. A significant O-PLS model was
332 obtained for the prediction of *APOA1BP* expression levels from the serum metabolic
333 profile (Figure 2a). Significant identified metabolites (Figure 2b) were further validated
334 by partial Spearman's correlation (Figure 2c). We identified asparagine, glycerol,
335 histidine, glycine, choline and citrate as positively associated with the expression of
336 *APOA1BP*, whereas glyceryl of lipids and very low level cholesterol in VLDL were
337 associated negatively. Metabolites associated positively with *APOA1BP* had negative
338 associations with atherosclerosis measures, particularly LmCCA (Figure 2g-i). We also
339 found a borderline significant negative ($r = -0.22$, $P = 0.051$) association between the
340 expression of *APOA1BP* and the inflammatory marker NAG. Metabolome-wide
341 association studies (MWAS) were also performed for the liver expression of *SREBF1* and

342 *SREBF2* using O-PLS multivariate regressions (Figure 2d,e and Supplementary Figure
343 3a) confirmed by partial Spearman's correlation (Figure 2 f and Supplementary Figure
344 3b). As expected, the expression of both genes was positively associated with several
345 lipids. They also had positive associations with inflammatory markers ~~†~~
346 ~~acetylglycoproteins~~ (NAG), branched-chain amino acids (BCAA) (valine, isoleucine)
347 and related catabolites (α -ketoisovalerate), lactate and proline. Most of these metabolites
348 had positive correlations with cIMT measures. In particular, BCAA had positive
349 associations with RICAe (Figure 2j-1), whereas NAG and α -ketoisovalerate had positive
350 associations with mCA ($R=0.27$, $P=0.028$; and $R=0.33$, $P=0.006$, respectively).

351

352 **ASSOCIATIONS OF HAEMATOPOIESIS AND LIPIDS WITH THE SERUM** 353 **METABOLIC PROFILES**

354 O-PLS regression models were also constructed to reveal associations between those
355 haematological and lipid parameters associated with the *APOA1BP-SREBF-NOTCH* axis
356 and the serum metabolome. A significant model with a strong predictive ability (Figure
357 3a) was obtained between the serum metabolic profile and the HDL-C levels. After
358 validation of the multivariate-identified metabolites by partial Spearman correlation,
359 metabolites associated with HDL-C were similar to those linked to *APOA1BP* and
360 *SREBF1* (Figure 3b). Hence, phosphocholine, choline, glycerol, and glycine, which
361 correlated positively with the expression of *APOA1BP*, also had a positive correlation
362 with HDL-C. Conversely, several lipids, inflammation-related metabolites (NAG),
363 BCAA (valine, isoleucine) and lactate, which were positively associated with *SREBF1*,
364 had a negative association with the circulating levels of HDL-C. Notably, the expression
365 of *NOTCH2NL* correlated negatively with the serum choline and phosphocholine levels

366 (Figure 3c,d) but positively with the BCAAs leucine and isoleucine (Figure 3e,f). It also
367 had a trend towards a positive association with NAG ($r = 0.20$, $P = 0.07$). A significant
368 O-PLS regression model was also obtained between the fasting serum TG levels and the
369 serum metabolome (Figure 3g). Patients with higher TG concentrations had higher levels
370 of several lipids, BCAAs and catabolites (isoleucine, α -ketoisovalerate), inflammation-
371 related metabolites (NAG), aspartate, proline, and acetone (Figure 3h). As expected, these
372 results agree with those metabolites positively associated with *SREBF1*. Interestingly,
373 several metabolites negatively associated with TG, including glycine, asparagine,
374 phosphocholine, glycerol, and histidine, were found to be positively associated with the
375 expression of *APOA1BP*. Finally, O-PLS regression models (Figure 3i) confirmed by
376 partial Spearman's correlation (Figure 3j) revealed that serum metabolites positively
377 associated with the leukocyte counts were similar to those associated with the expression
378 of *SREBF1*.

379

380 **Discussion**

381 Atherosclerosis and its progression is caused by lipid accumulation and local
382 inflammation of blood vessels, and is the major underlying cause of CVD. High plasma
383 concentrations of HDL have shown anti-atherogenic potential because HDL carries
384 excess cholesterol away from cells. Importantly, human studies have shown that HDL
385 cholesterol efflux capacity, a metric of HDL function that characterizes a key step in RCT,
386 may be athero-protective [1,3]. Recent *in vitro* and animal studies have shown that AIBP
387 may protect against atherosclerosis [5–8]. Here, we provided evidence for the first time,
388 to our knowledge, in humans of an inverse association between the expression of
389 *APOA1BP* and atherosclerosis measures.

390 *In vitro* studies have demonstrated a role of AIBP in promoting cholesterol efflux from
391 human umbilical vein endothelial cells to HDL and THP-1-derived macrophages, thereby
392 reducing lipid accumulation [5,6]. Mechanistically, AIBP enhances cholesterol efflux and
393 RCT by preventing ABCA1 protein degradation through facilitating its binding to
394 APOA1 on the cell membrane, thereby increasing ABCA1 levels [5]. Growing evidence
395 suggests that ABCA1 protects from atherosclerosis by exporting excess cholesterol from
396 cells to poorly lipidated APOA1, which is essential for the biogenesis of nascent HDL in
397 hepatocytes [23]. Recent animal studies have also highlighted the protection of AIBP
398 against atherosclerosis [7,8]. Hence, *ApoE*^{-/-} mice with established atherosclerosis and
399 treated with recombinant adeno-associated virus (rAAV) to overexpress AIBP showed
400 reduction of atherosclerotic plaque size and inflammation but increased circulating HDL
401 levels and RCT to the liver [8]. In the latter model, AIBP was overexpressed in the aorta
402 and peritoneal macrophages, but mainly in the liver. The striking increase in ABCA1
403 protein levels in the aortas and peritoneal macrophages of AIBP-treated mice suggests
404 again that the effects of AIBP are mediated through ABCA1. In another animal study,
405 *ApoA1bp*^{-/-}*Ldlr*^{-/-} mice fed a high-fat, high-cholesterol diet had exacerbated weight gain,
406 liver steatosis, hyperlipidaemia and atherosclerosis compared to *Ldlr*^{-/-} mice [7]. In
407 addition, AAV-mediated overexpression of AIBP in *Ldlr*^{-/-} mice protected against weight
408 gain, plasma lipid increase and atherosclerosis compared to controls.

409 In agreement with these results, we found negative associations between *APOA1BP*
410 expression levels and measures of cIMT. Conversely, we found a negative association
411 between the expression levels of *APOA1BP* and *ABCA1*. It is possible that in patients
412 with reduced hepatic *APOA1BP* expression, there is a compensatory response in the
413 expression of *ABCA1* to increase cholesterol efflux in the liver. In addition, although
414 treatment with AIBP increased ABCA1 protein levels in macrophages and *ApoE*^{-/-} mice,

415 it did not alter the ABCA1 mRNA expression [5,8]. In fact, ABCA1 protein levels and
416 mRNA expression are usually discordant as ABCA1 protein levels are regulated by a
417 diverse posttranscriptional mechanism [24]. In contrast to ABCA1, which is important
418 for the generation of nascent HDL, scavenger receptor class B member 1 (SR-BI) is a
419 receptor for mature HDL and mediates selective uptake of HDL cholesteryl esters into
420 the liver as the final step in RCT [25]. Consistently, we found a significant association
421 between *APOA1BP* and *SCARB1*, which encodes the SR-BI protein, which was opposite
422 to the *APOA1BP-ABCA1* correlation.

423 In addition to the ABCA1 transporter pathway, the VLDL-APOB secretion pathway has
424 been proposed as the major pathway for the secretion of cholesterol from hepatocytes
425 together with TG into plasma [26]. Interestingly, the VLDL secretion pathway is
426 modulated by SREBP1c [27], encoded by *SREBF1*, which we found strongly positively
427 associated with atherosclerosis. Specifically, *SREBF1* correlated with cIMT measures in
428 all segments of the left carotid artery, which is in agreement the higher vulnerability of
429 the left carotid artery to atherosclerosis [28,29].—Hepatic expression of SREBP1c is also
430 increased in hepatic steatosis [30], which is consistent with our results. A recent study in
431 zebrafish has shown that *Aibp2*-mediated HPSC expansion through the up-regulation of
432 *Sreb2* (but not *Sreb1*), which predominantly regulates cholesterol synthesis [14].
433 Although we mainly found *SREBF1* associated with cIMT rather than *SREBF2*, it is worth
434 noting that *SREBF1* is transcribed into two variants: SREBP-1c, which solely regulates
435 lipid synthesis, and SREBP-1a, which controls both cholesterol and lipid synthesis. AIBP
436 also seem to modulate Notch signalling in mice and zebrafish [13,14]. In agreement with
437 these results, we found strong associations between the expression of *APOA1BP* and the
438 expression of all Notch signalling receptors and jagged ligands, but not with delta-like
439 ligands. Interestingly, jagged and delta-like ligands have shown opposite effects on

440 angiogenesis and regulation of T cells [31,32]. Consistent with a higher susceptibility of
441 the left carotid artery, w~~Although we also~~ found that *NOTCH1* and *NOTCH4* were
442 positively associated with left cIMT measures~~atherosclerosis~~. Despite these associations,
443 ~~it is particularly noticeable that the expression of human-specific gene~~ *NOTCH2NL* had
444 the strongest associations with atherosclerotic measures. Interestingly, among all genes
445 involved in cholesterol metabolism, *NOTCH2NL* had the strongest positive association
446 with *ABCA1*, suggesting again a potential upregulation of *ABCA1* expression to increase
447 cholesterol efflux in patients with cIMT. Little is known about *NOTCH2NL*, but it has
448 recently stood out for its ability to enhance Notch signalling and expand human cortical
449 progenitor cells [33,34]. Consistent with this link between cholesterol metabolism and
450 haematopoiesis, we found significant associations among the expression of *APOA1BP*,
451 *SREBF1* and *NOTCH2NL*, and haematology and lipid parameters.

452 We found that the expression of transcripts *APOA1BP*, *SREBF1*, *SREBF2* and
453 *NOTCH2NL* was associated with several plasma metabolites. *APOA1BP* had positive
454 correlations with three amino acids (asparagine, histidine, glycine), glycerol, choline and
455 citrate. These amino acids were also associated positively with circulating HDL-C levels,
456 but negatively with TG and WBC counts. Glycine, histidine and asparagine were also
457 negatively associated with cIMT measures. Of note, among 35 plasma metabolites
458 quantified in 1049 individuals without coronary artery disease (CAD) and diabetes,
459 histidine was most strongly associated with lower risk for incident CAD, followed by
460 asparagine [35]. Low circulating levels of glycine have also been causally associated with
461 higher incidence of coronary heart disease [36].

462 *APOA1BP* expression also had a positive association with choline. Remarkably, both
463 choline and phosphocholine levels had very strong positive associations with HDL-C but
464 correlated negatively with the expression of *NOTCH2NL*. There is evidence suggesting a

465 connection between choline and HDL metabolism. Hence, phosphatidylcholine is the
466 major phospholipid component of all plasma lipoproteins and the biosynthesis of
467 phosphatidylcholine in the liver is critical for the synthesis and secretion of HDL and
468 VLDL [37]. Interestingly, *APOA1BP* correlated negatively with the expression of liver
469 enzymes involved in the synthesis of phosphatidylcholine from choline and
470 phosphocholine, suggesting an up-regulation of the synthesis of phosphatidylcholine in
471 patients with lower *APOA1BP* to increase assembly and clearance of lipoproteins. Due to
472 the role of lecithin–cholesterol acyltransferase (*LCAT*) in the formation of HDL and
473 RCT, we also assessed the relation between the expression levels of *APOA1BP* and *LCAT*
474 and found a positive association ($R=0.27$, $P=0.01$). Interestingly, although studies in the
475 general population gave inconsistent results, patients with *LCAT* deficiency have shown
476 a significant increase in the incidence of CVD [38]. Despite the associations with
477 *APOA1BP* and HDL, neither choline nor phosphocholine had associations with measures
478 of atherosclerosis. Previous studies have shown inconsistent associations between
479 circulating choline and phosphocholine levels and cardiovascular events. Both
480 metabolites were positively associated with the risk of CVD and stroke after 4.8 years of
481 follow-up in participants at high cardiovascular risk within the PREDIMED study, but no
482 associations were found between 1-year changes in these metabolites and the incidence
483 of CVD [39]. Similarly, higher plasma choline levels were associated with increased risk
484 of major cardiac events after 3 years of follow-up in patients undergoing elective
485 diagnostic coronary angiography, but they did not predict risk when trimethylamine *N*-
486 oxide, a choline metabolite, was added to the model [40]. In cross-section studies higher
487 plasma choline concentrations have been associated with an unfavourable
488 cardiometabolic risk factor profile, including lower HDL levels [41,42]. However, it is
489 worth noting that plasma choline levels do not reflect choline status because disturbances

490 in circulating choline arise early in disease development [43,44] and circulating levels
491 may depend on lipid overload. In this sense, plasma choline metabolites differed between
492 normal and overweight men [45]. In addition, both low and high plasma concentrations
493 may be associated with adverse effects [46].

494 As expected, the expression levels of *SREBF1* and *SREBF2* had positive associations with
495 several lipids. These genes also correlated positively with circulating levels of BCAA and
496 catabolites, NAG and lactate. Except for lactate, we found that these metabolites were all
497 positively associated with measure of cIMT. Several cross-section and prospective cohort
498 studies revealed positive associations of BCAA with major metabolic disorders [47] and
499 recently they have also been positively associated with risk factors of CAD, in particular
500 cIMT [48]. Interestingly, we also found a positive correlation between the expression
501 levels of *NOTCH2NL* and BCAA. In line with atherosclerosis being a chronic
502 inflammatory disorder, we found a consistent association between NAG, a novel marker
503 of chronic inflammation [22], and cIMT measures. Consistently, we found that NAG
504 levels were the strongest predictors of WBC counts, which also had positive associations
505 with BCAA. Supporting the role of the *APOA1BP-SREBF-NOTCH* axis and
506 inflammation in atherosclerosis, we also found that NAG levels were negatively
507 associated with the expression of *APOA1BP*, but positively with that of *SREBF1*,
508 *SREBF2*, and *NOTCH2NL*. Finally, most of the metabolites associated with *SREBF1* and
509 *SREBF2* had similar associations with TG, but opposite to those of HDL.

510 The main limitation of our study is its cross-sectional nature. Therefore, we cannot infer
511 cause-effect relationships. Second, the results cannot be extrapolated to the general
512 population, as subjects in the current study were morbidly obese. In addition, we did not
513 measure AIBP protein levels. The strengths of the present work include the use of two
514 independent well-characterized cohorts, which allowed the control for potential

515 confounders, with comprehensive metabolomic, transcriptomic, liver biopsy and cIMT
516 data.

517 In conclusion, our findings demonstrate, for the first time, an atheroprotective association
518 between the expression levels of *APOA1BP* and atherosclerosis in humans. We have also
519 shown a connection between *APOA1BP*, Notch signalling and inflammation with
520 atherosclerosis.

521

522 **Acknowledgments**

523 This work was supported by EU-FP7 FLORINASH (Health-F2-2009-241913) to R.B.,
524 M.F., J.M.F.R. Infrastructure support was provided by the National Institute for Health
525 Research (NIHR) Imperial Biomedical Research Centre (BRC). J.M.-P. is funded by the
526 Instituto de Salud Carlos III (Madrid, Spain) through a Miguel Servet programme
527 (CP18/00009). L.H. was in receipt of an MRC Intermediate Research Fellowship (UK
528 MED-BIO; grant number MR/L01632X/1).

529 **References**

- 530 [1] Khera A V., Cuchel M, de la Llera-Moya M, Rodrigues A, Burke MF, Jafri K, et
531 al. Cholesterol Efflux Capacity, High-Density Lipoprotein Function, and
532 Atherosclerosis. *N Engl J Med* 2011;364:127–35. doi:10.1056/NEJMoa1001689.
- 533 [2] Ohashi R, Mu H, Wang X, Yao Q, Chen C. Reverse cholesterol transport and
534 cholesterol efflux in atherosclerosis. *QJM An Int J Med* 2005;98:845–56.
535 doi:10.1093/qjmed/hci136.
- 536 [3] Rohatgi A, Khera A, Berry JD, Givens EG, Ayers CR, Wedin KE, et al. HDL
537 Cholesterol Efflux Capacity and Incident Cardiovascular Events. *N Engl J Med*
538 2014;371:2383–93. doi:10.1056/NEJMoa1409065.
- 539 [4] Ritter M, Buechler C, Boettcher A, Barlage S, Schmitz-Madry A, Orsó E, et al.
540 Cloning and Characterization of a Novel Apolipoprotein A-I Binding Protein, AI-
541 BP, Secreted by Cells of the Kidney Proximal Tubules in Response to HDL or
542 ApoA-I. *Genomics* 2002;79:693–702. doi:10.1006/geno.2002.6761.
- 543 [5] Zhang M, Li L, Xie W, Wu J-F, Yao F, Tan Y-L, et al. Apolipoprotein A-1
544 binding protein promotes macrophage cholesterol efflux by facilitating
545 apolipoprotein A-1 binding to ABCA1 and preventing ABCA1 degradation.
546 *Atherosclerosis* 2016;248:149–59. doi:10.1016/j.atherosclerosis.2016.03.008.
- 547 [6] Fang L, Choi S-H, Baek JS, Liu C, Almazan F, Ulrich F, et al. Control of
548 angiogenesis by AIBP-mediated cholesterol efflux. *Nature* 2013;498:118–22.
549 doi:10.1038/nature12166.
- 550 [7] Schneider DA, Choi S-H, Agatista-Boyle C, Zhu L, Kim J, Pattison J, et al. AIBP
551 protects against metabolic abnormalities and atherosclerosis. *J Lipid Res*

Formatted: Spanish (Spain)

- 552 2018;59:854–63. doi:10.1194/jlr.M083618.
- 553 [8] Zhang M, Zhao G-J, Yao F, Xia X-D, Gong D, Zhao Z-W, et al. AIBP reduces
554 atherosclerosis by promoting reverse cholesterol transport and ameliorating
555 inflammation in apoE ^{-/-} mice. *Atherosclerosis* 2018;273:122–30.
556 doi:10.1016/j.atherosclerosis.2018.03.010.
- 557 [9] Gisterå A, Hansson GK. The immunology of atherosclerosis. *Nat Rev Nephrol*
558 2017;13:368–80. doi:10.1038/nrneph.2017.51.
- 559 [10] Radtke F, MacDonald HR, Tacchini-Cottier F. Regulation of innate and adaptive
560 immunity by Notch. *Nat Rev Immunol* 2013;13:427–37. doi:10.1038/nri3445.
- 561 [11] Vieceli Dalla Sega F, Fortini F, Aquila G, Campo G, Vaccarezza M, Rizzo P.
562 Notch Signaling Regulates Immune Responses in Atherosclerosis. *Front*
563 *Immunol* 2019;10. doi:10.3389/fimmu.2019.01130.
- 564 [12] Soehnlein O, Swirski FK. Hypercholesterolemia links hematopoiesis with
565 atherosclerosis. *Trends Endocrinol Metab* 2013;24:129–36.
566 doi:10.1016/j.tem.2012.10.008.
- 567 [13] Mao R, Meng S, Gu Q, Araujo-Gutierrez R, Kumar S, Yan Q, et al. AIBP Limits
568 Angiogenesis Through γ -Secretase-Mediated Upregulation of Notch Signaling.
569 *Circ Res* 2017;120:1727–39. doi:10.1161/CIRCRESAHA.116.309754.
- 570 [14] Gu Q, Yang X, Lv J, Zhang J, Xia B, Kim J, et al. AIBP-mediated cholesterol
571 efflux instructs hematopoietic stem and progenitor cell fate. *Science* (80-)
572 2019;363:1085–8. doi:10.1126/science.aav1749.
- 573 [15] Muench MO, Beyer AI, Fomin ME, Thakker R, Mulvaney US, Nakamura M, et

- 574 al. The Adult Livers of Immunodeficient Mice Support Human Hematopoiesis:
575 Evidence for a Hepatic Mast Cell Population that Develops Early in Human
576 Ontogeny. *PLoS One* 2014;9:e97312. doi:10.1371/journal.pone.0097312.
- 577 [16] Golden-Mason L, O'Farrelly C. Having it all? Stem cells, haematopoiesis and
578 lymphopoiesis in adult human liver. *Immunol Cell Biol* 2002;80:45–51.
579 doi:10.1046/j.1440-1711.2002.01066.x.
- 580 [17] Hoyles L, Fernández-Real J-M, Federici M, Serino M, Abbott J, Charpentier J, et
581 al. Molecular phenomics and metagenomics of hepatic steatosis in non-diabetic
582 obese women. *Nat Med* 2018;24:1070–80. doi:10.1038/s41591-018-0061-3.
- 583 [18] Kleiner DE, Brunt EM, Van Natta M, Behling C, Contos MJ, Cummings OW, et
584 al. Design and validation of a histological scoring system for nonalcoholic fatty
585 liver disease. *Hepatology* 2005;41:1313–21. doi:10.1002/hep.20701.
- 586 [19] Fleige S, Pfaffl MW. RNA integrity and the effect on the real-time qRT-PCR
587 performance. *Mol Aspects Med* 2006;27:126–39.
588 doi:10.1016/j.mam.2005.12.003.
- 589 [20] Smyth GK. *limma: Linear Models for Microarray Data*. *Bioinforma. Comput.*
590 *Biol. Solut. Using R Bioconductor*, New York: Springer-Verlag; 2005, p. 397–
591 420. doi:10.1007/0-387-29362-0_23.
- 592 [21] Touboul P-J, Hennerici MG, Meairs S, Adams H, Amarenco P, Bornstein N, et
593 al. Mannheim carotid intima-media thickness and plaque consensus (2004-2006-
594 2011). An update on behalf of the advisory board of the 3rd, 4th and 5th
595 watching the risk symposia, at the 13th, 15th and 20th European Stroke
596 Conferences, Mannheim, Germany, 2004, Brussels, Belgium, 2006, and

- 597 Hamburg, Germany, 2011. *Cerebrovasc Dis* 2012;34:290–6.
598 doi:10.1159/000343145.
- 599 [22] Connelly MA, Otvos JD, Shalaurova I, Playford MP, Mehta NN. GlycA, a novel
600 biomarker of systemic inflammation and cardiovascular disease risk. *J Transl*
601 *Med* 2017;15:219. doi:10.1186/s12967-017-1321-6.
- 602 [23] Wang S, Smith JD. ABCA1 and nascent HDL biogenesis. *BioFactors*
603 2014;40:547–54. doi:10.1002/biof.1187.
- 604 [24] Lv Y, Yin K, Fu Y, Zhang D, Chen W, Tang C. Posttranscriptional Regulation of
605 *ATP-Binding Cassette Transporter A1* in Lipid Metabolism. *DNA Cell Biol*
606 2013;32:348–58. doi:10.1089/dna.2012.1940.
- 607 [25] Hoekstra M. SR-BI as target in atherosclerosis and cardiovascular disease - A
608 comprehensive appraisal of the cellular functions of SR-BI in physiology and
609 disease. *Atherosclerosis* 2017;258:153–61.
610 doi:10.1016/j.atherosclerosis.2017.01.034.
- 611 [26] Shelness GS, Sellers JA. Very-low-density lipoprotein assembly and secretion.
612 *Curr Opin Lipidol* 2001;12:151–7.
- 613 [27] Okazaki H, Goldstein JL, Brown MS, Liang G. LXR-SREBP-1c-phospholipid
614 transfer protein axis controls very low density lipoprotein (VLDL) particle size. *J*
615 *Biol Chem* 2010;285:6801–10. doi:10.1074/jbc.M109.079459.
- 616 [28] Selwaness M, Van Den Bouwhuijsen Q, Van Onkelen RS, Hofman A, Franco
617 OH, Van Der Lugt A, et al. Atherosclerotic plaque in the left carotid artery is
618 more vulnerable than in the right. *Stroke* 2014;45:3226–30.
619 doi:10.1161/STROKEAHA.114.005202.

Formatted: Spanish (Spain)

- 620 [29] Chou CL, Wu YJ, Hung CL, Liu CC, Wang S De, Wu TW, et al. Segment-
621 specific prevalence of carotid artery plaque and stenosis in middle-aged adults
622 and elders in Taiwan: A community-based study. *J Formos Med Assoc*
623 2019;118:64–71. doi:10.1016/j.jfma.2018.01.009.
- 624 [30] Ferré P, Fougère F. Hepatic steatosis: a role for de novo lipogenesis and the
625 transcription factor SREBP-1c. *Diabetes, Obes Metab* 2010;12:83–92.
626 doi:10.1111/j.1463-1326.2010.01275.x.
- 627 [31] Rutz S, Mordmüller B, Sakano S, Scheffold A. Notch ligands Delta-like1, Delta-
628 like4 and Jagged1 differentially regulate activation of peripheral T helper cells.
629 *Eur J Immunol* 2005;35:2443–51. doi:10.1002/eji.200526294.
- 630 [32] Benedito R, Roca C, Sörensen I, Adams S, Gossler A, Fruttiger M, et al. The
631 notch ligands Dll4 and Jagged1 have opposing effects on angiogenesis. *Cell*
632 2009;137:1124–35. doi:10.1016/j.cell.2009.03.025.
- 633 [33] Fiddes IT, Lodewijk GA, Mooring M, Bosworth CM, Ewing AD, Mantalas GL,
634 et al. Human-Specific NOTCH2NL Genes Affect Notch Signaling and Cortical
635 Neurogenesis. *Cell* 2018;173:1356–1369.e22. doi:10.1016/j.cell.2018.03.051.
- 636 [34] Suzuki IK, Gacquer D, Van Heurck R, Kumar D, Wojno M, Bilheu A, et al.
637 Human-Specific NOTCH2NL Genes Expand Cortical Neurogenesis through
638 Delta/Notch Regulation. *Cell* 2018;173:1370–1384.e16.
639 doi:10.1016/j.cell.2018.03.067.
- 640 [35] Ottosson F, Smith E, Melander O, Fernandez C. Altered Asparagine and
641 Glutamate Homeostasis Precede Coronary Artery Disease and Type 2 Diabetes. *J*
642 *Clin Endocrinol Metab* 2018;103:3060–9. doi:10.1210/jc.2018-00546.

- 643 [36] Wittemans LBL, Lotta LA, Oliver-Williams C, Stewart ID, Surendran P,
644 Karthikeyan S, et al. Assessing the causal association of glycine with risk of
645 cardio-metabolic diseases. *Nat Commun* 2019;10:1060. doi:10.1038/s41467-019-
646 08936-1.
- 647 [37] Cole LK, Vance JE, Vance DE. Phosphatidylcholine biosynthesis and lipoprotein
648 metabolism. *Biochim Biophys Acta - Mol Cell Biol Lipids* 2012;1821:754–61.
649 doi:10.1016/j.bbalip.2011.09.009.
- 650 [38] Ossoli A, Simonelli S, Vitali C, Franceschini G, Calabresi L. Role of LCAT in
651 Atherosclerosis. *J Atheroscler Thromb* 2016;23:119–27. doi:10.5551/jat.32854.
- 652 [39] Guasch- Ferré M, Hu FB, Ruiz- Canela M, Bulló M, Toledo E, Wang DD, et al.
653 Plasma Metabolites From Choline Pathway and Risk of Cardiovascular Disease
654 in the PREDIMED (Prevention With Mediterranean Diet) Study. *J Am Heart*
655 *Assoc* 2017;6. doi:10.1161/JAHA.117.006524.
- 656 [40] Wang Z, Tang WHW, Buffa JA, Fu X, Britt EB, Koeth RA, et al. Prognostic
657 value of choline and betaine depends on intestinal microbiota-generated
658 metabolite trimethylamine-N-oxide. *Eur Heart J* 2014;35:904–10.
659 doi:10.1093/eurheartj/ehu002.
- 660 [41] Roe AJ, Zhang S, Bhadelia RA, Johnson EJ, Lichtenstein AH, Rogers GT, et al.
661 Choline and its metabolites are differently associated with cardiometabolic risk
662 factors, history of cardiovascular disease, and MRI-documented cerebrovascular
663 disease in older adults. *Am J Clin Nutr* 2017;105:1283–90.
664 doi:10.3945/ajcn.116.137158.
- 665 [42] Konstantinova S V., Tell GS, Vollset SE, Nygård O, Bleie Ø, Ueland PM.

- 666 Divergent Associations of Plasma Choline and Betaine with Components of
667 Metabolic Syndrome in Middle Age and Elderly Men and Women. *J Nutr*
668 2008;138:914–20. doi:10.1093/jn/138.5.914.
- 669 [43] Fischer LM, daCosta KA, Kwock L, Stewart PW, Lu T-S, Stabler SP, et al. Sex
670 and menopausal status influence human dietary requirements for the nutrient
671 choline. *Am J Clin Nutr* 2007;85:1275–85. doi:10.1093/ajcn/85.5.1275.
- 672 [44] Bae S, Ulrich CM, Neuhauser ML, Malysheva O, Bailey LB, Xiao L, et al.
673 Plasma choline metabolites and colorectal cancer risk in the Women’s Health
674 Initiative Observational Study. *Cancer Res* 2014;74:7442–52. doi:10.1158/0008-
675 5472.CAN-14-1835.
- 676 [45] Yan J, Winter LB, Burns-Whitmore B, Vermeulen F, Caudill MA. Plasma
677 choline metabolites associate with metabolic stress among young overweight
678 men in a genotype-specific manner. *Nutr Diabetes* 2012;2:e49.
679 doi:10.1038/nutd.2012.23.
- 680 [46] Lever M, George PM, Atkinson W, Molyneux SL, Elmslie JL, Slow S, et al.
681 Plasma Lipids and Betaine Are Related in an Acute Coronary Syndrome Cohort.
682 *PLoS One* 2011;6:e21666. doi:10.1371/journal.pone.0021666.
- 683 [47] Zhang Z-Y, Monleon D, Verhamme P, Staessen JA. Branched-Chain Amino
684 Acids as Critical Switches in Health and Disease. *Hypertension* 2018;72:1012–
685 22. doi:10.1161/HYPERTENSIONAHA.118.10919.
- 686 [48] Yang R, Dong J, Zhao H, Li H, Guo H, Wang S, et al. Association of branched-
687 chain amino acids with carotid intima-media thickness and coronary artery
688 disease risk factors. *PLoS One* 2014;9:e99598.

689 [doi:10.1371/journal.pone.0099598](https://doi.org/10.1371/journal.pone.0099598).

690

691 **Figure Legends**

692 **Figure 1. Associations of expression levels of *APOA1BP*, *SREBFs*, and *NOTCHs* genes**
693 **with cIMT, steatosis, haematology and lipid measures and cholesterol and notch**
694 **pathway genes. a)** Heatmap displaying the partial Spearman's correlation coefficients
695 (adjusted for age, BMI, sex, and cohort) between genes and cIMT measures. * $p < 0.05$,
696 ** $p < 0.01$, *** $p < 0.001$. **b)** Association of expression levels of *SREBF1* with the steatosis
697 degree (ANCOVA and Tukey-kramer tests). **c)** Cholesterol metabolism pathway genes
698 significantly associated with mean CCA based on partial Spearman's correlation adjusted
699 for age, BMI, sex, and cohort. **d-i)** Scatter plots between expression levels of selected
700 genes and haematological and lipid parameters. Partial Spearman's correlation and
701 significance values adjusted for age, BMI, sex, and cohort are shown. **j-k)** Permutation
702 test for the goodness-of-fit (R^2Y) and goodness of prediction (Q^2Y) obtained from the O-
703 PLS models between the expression levels of *APOA1BP* and the expression levels of
704 genes involved in the Notch signalling and cholesterol pathways, respectively. **l-m)**
705 Significant Notch and cholesterol pathway genes associated with *APOA1BP* after further
706 validation of the O-PLS identified genes by partial Spearman's correlation adjusting for
707 age, sex, BMI, and country.

708 **Figure 2. Associations of metabolomics data with the expression levels of *APOA1BP*,**
709 ***SREBF1*, and cIMT measures. a)** Permutation test for the goodness-of-fit (R^2Y) and
710 goodness of prediction (Q^2Y) obtained from the O-PLS models between the expression
711 levels of *APOA1BP* and the serum metabolome. **b)** Significant serum metabolites
712 obtained from the O-PLS model. Statistically significant metabolites are coloured in red
713 if positively associated with *APOA1BP* and blue if negatively associated. **c)** Metabolites
714 associated with *APOA1BP* after further validation of the O-PLS identified metabolites by
715 partial Spearman's correlation adjusting for age, sex, BMI, and country. **d)** Permutation

716 test for the goodness-of-fit (R^2Y) and goodness of prediction (Q^2Y) obtained from the O-
717 PLS models between the expression levels of *SREBF1* and the serum metabolome. **e)**
718 Significant serum metabolites obtained from the O-PLS model. Statistically significant
719 metabolites are coloured in red if positively associated with *SREBF1* and blue if
720 negatively associated. **f)** Metabolites associated with *SREBF1* after further validation of
721 the O-PLS identified metabolites by partial Spearman's correlation adjusting for age, sex,
722 BMI, and country. **g-l)** Scatter plots between selected metabolites and cIMT measures.
723 Partial Spearman's correlation and significance values adjusted for age, BMI, sex, and
724 cohort are shown.

725 **Figure 3. Associations of metabolomics data with the lipid parameters, WBC, and**
726 ***NOTCH2NL* expression levels.** **a)** Permutation test for the goodness-of-fit (R^2Y) and
727 goodness of prediction (Q^2Y) obtained from the O-PLS models between the expression
728 levels of HDL-C and the serum metabolome. **b)** Metabolites associated with HDL-C after
729 further validation of the O-PLS identified metabolites by partial Spearman's correlation
730 adjusting for age, sex, BMI, and country. **c-f)** Scatter plots between selected metabolites
731 and *NOTCH2NL* expression levels. Partial Spearman's correlation and significance
732 values adjusted for age, BMI, sex, and cohort are shown. **g)** Permutation test for the
733 goodness-of-fit (R^2Y) and goodness of prediction (Q^2Y) obtained from the O-PLS models
734 between the expression levels of TG and the serum metabolome. **h)** Metabolites
735 associated with TG after further validation of the O-PLS identified metabolites by partial
736 Spearman's correlation adjusting for age, sex, BMI, and country. **i)** Permutation test for
737 the goodness-of-fit (R^2Y) and goodness of prediction (Q^2Y) obtained from the O-PLS
738 models between the expression levels of WBC and the serum metabolome. **j)** Metabolites
739 associated with WBC after further validation of the O-PLS identified metabolites by
740 partial Spearman's correlation adjusting for age, sex, BMI, and country.

741 **Supplementary Figure 1. a)** Cholesterol metabolism pathway genes significantly
742 associated with mean CA based on partial Spearman's correlation adjusted for age, BMI,
743 sex, and cohort. **b)** Heatmap displaying the partial Spearman's correlations (adjusted for
744 age, BMI, sex, and cohort) between cIMT measures and inflammation measured by NMR
745 plasma levels of N-acetylglycoproteins (NAG). **c)** Heatmap displaying the partial
746 Spearman's correlation coefficients (adjusted for age, BMI, sex, and cohort) between
747 genes and haematological parameters. **d)** Heatmap displaying the partial Spearman's
748 correlation coefficients (adjusted for age, BMI, sex, and cohort) between haematological
749 parameters and cIMT measures.

750 **Supplementary Figure 2. a,b)** Permutation test for the goodness-of-fit (R^2Y) and
751 goodness of prediction (Q^2Y) obtained from the O-PLS models between the expression
752 levels of *SREBF1* and the expression levels of genes involved in Notch signalling and
753 cholesterol synthesis pathways, respectively. **c,d)** Significant Notch signalling and
754 cholesterol pathway genes associated with *SREBF1* after further validation of the O-PLS
755 identified genes by partial Spearman's correlation adjusting for age, sex, BMI, and
756 country, respectively. **ea)** Permutation test for the goodness-of-fit (R^2Y) and goodness of
757 prediction (Q^2Y) obtained from the O-PLS models between the expression levels of
758 *NOTCH2NL* and the expression levels of genes involved in cholesterol synthesis
759 pathway. **fb)** Significant cholesterol pathway genes associated with *NOTCH2NL* after
760 further validation of the O-PLS identified genes by partial Spearman's correlation
761 adjusting for age, sex, BMI, and country.

762 **Supplementary Figure 3. a)** Permutation test for the goodness-of-fit (R^2Y) and goodness
763 of prediction (Q^2Y) obtained from the O-PLS models between the expression levels of
764 *SREBF2* and the serum metabolome. **b)** Significant serum metabolites obtained from the
765 O-PLS model. Statistically significant metabolites are coloured in red if positively

766 associated with *SREBF2* and blue if negatively associated. c) Metabolites associated with
767 *SREBF2* after further validation of the O-PLS identified metabolites by partial
768 Spearman's correlation adjusting for age, sex, BMI, and country

769

Table 1. Baseline characteristics of participants.

Variables	All (n=78)
Age (years)	42.4 ± 1.16
BMI (kg/m ²)	46.2 (42.4-51.1)
Waist circumference (cm)	127.0 (119.5-138.0)
Sex (women, %)	79.2
SBP (mmHg)	134.0 (122.5-144.0)
DBP (mmHg)	81.0 (75.0-90.0)
Biochemistry	
Glucose (mg/dL)	95.0 (88.5-101.5)
HOMA-IR	4.50 (2.95-6.90)
Triglycerides (mg/dL)	112.0 (82.0-143.5)
Total cholesterol (mg/dL)	197.5 ± 4.6
LDL cholesterol (mg/dL)	131.0 ± 4.0
HDL cholesterol (mg/dL)	45.0 (40.0-51.2)
Haematology	
Eosinophils	150.0 (100.0-200.0)
Neutrophils	4810 (3665-5795)
Lymphocytes	2360 ± 86.9
Monocytes	500 (420-600)
Total WBC	7350 (6385-9030)
RBC	4.66 (4.46-4.91)
Liver	
HsCRP	0.88 (0.47-1.39)
AST	19.0 (15.0-28.0)
ALT	30.0 (22.0-43.5)
Steatosis grade (%):	
Grade 0	15.6
Grade 1	33.8
Grade 2	24.7
Grade 3	26.0
Atherosclerosis	
RproCCAi	0.70 (0.60-0.80)
RproCCAe	0.70 (0.60-0.80)
RpreCCAi	0.79 ± 0.03
RpreCCAe	0.72 (0.60-0.80)
RICAi	0.70 (0.60-0.90)
RICAe	0.70 (0.54-0.85)
mRCCA	0.73 ± 0.02
mRICA	0.71 ± 0.02
LproCCAi	0.70 (0.60-0.85)
LproCCAe	0.69 (0.60-0.80)
LpreCCAi	0.80 (0.70-1.0)
LpreCCAe	0.84 ± 0.03
LICAi	0.77 (0.57-0.90)
LICAe	0.70 (0.60-0.87)
mLCCA	0.76 ± 0.02
mLICA	0.73 ± 0.03
mCCA	0.74 ± 0.02
mCA	0.73 ± 0.02

771 Values are expressed as means ± SEM for normally distributed variables and median [IQR] for non-normally
772 distributed variables. ALT, alanine aminotransferase; AST, aspartate aminotransferase; HsCRP, high sensitivity

773 C-reactive protein; e, external; i, internal; ICA, internal carotid artery; L, left; m, mean; preCCA, pre bifurcation
774 common carotid artery; proCCA, proximal segment common carotid artery; R, right; RBC, red blood cells; WBC,
775 white blood cells.

1 Reference: YCLNU-D-19-01600

2

3 Title: **The APOA1BP-SREBF-NOTCH axis is associated with reduced atherosclerosis**
4 **risk**

5 **General comments to the reviewers**

6 We greatly appreciate all the comments and suggestions made by the reviewers, the
7 responses to which strengthen our manuscript. We have revised and modified the
8 manuscript according to these suggestions, as detailed below.

9

10 **Responses to Reviewer 1**

11

12 *Reviewer #1: The manuscript titled "The APOA1B-SREBF-NOTCH axis is associated with*
13 *reduced atherosclerosis risk," is interesting and clearly written. It has a novelty because*
14 *the authors tried to elucidate the association between APOA1B-SREBF-NOTCH axis and*
15 *atherosclerosis in humans. However, the reviewer has several concerns regarding this*
16 *article. Specific comments are as follows.*

17

18 *Major points:*

19

20 1. *The authors demonstrated the possible relations between APOA1B and SREBF, and*
21 *between APOA1B and NOTCH. However, the reviewer cannot find the data showing the*
22 *relation between SREBF-NOTCH. Since the authors claim "the APOA1B-SREBF-NOTCH*
23 *axis", they should show clearly the relation between SREBF-NOTCH. We thank the*
24 **reviewer for this comment and we agree with him that we had not shown a clear**
25 **evidence for the relation between SREBF and NOTCH signalling. Therefore, similar**
26 **to what we did for the associations between APOA1BP expression and Notch and**
27 **cholesterol pathway associated genes, we built O-PLS models between the expression**
28 **of SREBF1 and Notch and cholesterol genes, respectively. In both cases, we obtained**
29 **significant models ($P < 0.001$) associating SREBF1 with Notch and cholesterol**

30 pathways. Both models were further validated by partial Spearman's correlation
31 adjusting for age, sex, BMI, and country. Interestingly, the expression of *SREBF1*
32 was positively associated with both *NOTCH1* and *ABCA1* expression, which we had
33 found negatively associated with *APOA1BP*. In the case of *SREBF2*, however, we did
34 not find significant associations with the Notch pathway genes. We have added all
35 these results in the results section and we have created a new Supplementary Figure
36 2.

37

38 2. *In this study, the authors investigate morbidly obese population only, however, the*
39 *title does not imply this specific population. The reviewer feels this could be misleading for*
40 *the readers. We agree with the reviewer that the title lacks information about the*
41 *study population and it can be misleading. We have added this information in the*
42 *title and now it reads as: "The APOA1BP-SREBF-NOTCH axis is associated with*
43 *reduced atherosclerosis risk in morbidly obese patients".*

44

45

46 *Minor points:*

47

48 1. *The O-PLS regression model figures are difficult to understand because those figures*
49 *do not have adequate variables information. Please refer to figure 1j-k, 2a-b, 2d-e, 3a, 3g,*
50 *3i, Supplemental figure 2a and Supplemental figures 3a-b. It would be easier to*
51 *understand if these figures contain adequate information regarding the variables. We*
52 **agree with the reviewer that the figures are no straightforwardly understandable**
53 **without reading the figure legends. Following reviewer's suggestion, we have added**
54 **in each figure the variables X and Y involved in the corresponding model.**

55

56 2. *The reviewer found mistyping which is mentioned below:*

57 *Page 13, line 280, "RproCAAi" should be "RproCCAi". Corrected*

58 *Page 22, line 507, "APO1BP" should be "APOA1BP". Corrected*

59

60 **Responses to Reviewer 2**

61

62 *Reviewer #2: Mayneris-Perxachs, et al. investigated correlation between gene expression*
63 *in the liver (e.g., APOA1BP, SREBF, and Notch) and carotid atherosclerosis in morbidly*
64 *obese patients. The authors employed sophisticated methods such as metabolomics*
65 *analyses and transcriptomic analyses, and suggested "APOA1BP-SREBF-NOTCH axis*
66 *signaling pathway" and its association with atherosclerosis.*

67 *This reviewer has following comments to this study.*

68 *1. The mechanisms by which APOA1BP-SREBF-NOTCH axis signaling pathway affect*
69 *atherogenesis is not clear. How the difference in gene expression in the liver links with the*
70 *carotid artery atherosclerosis?*

71 **Recent evidence suggests that cholesterol pathways link hematopoiesis with**
72 **atherosclerosis, with an interesting role for the AIBP-SREBP-NOTCH axis. The**
73 **bone marrow is the main site of haematopoiesis in adults. However, the liver is the**
74 **main site in prenatal development and some studies have provided evidence that it is**
75 **still active in adults. Therefore, we hypothesized that the gene expression in the liver**
76 **could be related to cholesterol metabolism and atherosclerosis. Thus, our aim was to**
77 **show for the first time in humans an association of the APOA1BP-SREBF-NOTCH**
78 **axis with atherosclerosis. We have to take into account that we have analysed cross-**
79 **sectional data. Therefore, we cannot infer causality or describe mechanisms, but just**
80 **associations. In zebrafish, increased cholesterol efflux mediated by Aibp2 has shown**
81 **to activate Srebp2, which in turn upregulated Notch resulting in an expansion of**
82 **hematopoietic stem and progenitor cells (HPSC) in the bone marrow. In human**
83 **subjects with hypercholesterolemia (the driving force for atherosclerosis) they found**
84 **that the number of HPSC are elevated and SREBP and NOTCH are upregulated in**
85 **HPSC isolated from these subjects. Here, we also found positive associations between**
86 **SREBF1, SREBF2 and NOTCH2NL expression and atherosclerosis parameters and**
87 **blood cells, whereas APOA1BP had opposite associations. We also found associations**
88 **among APOA1BP, Notch pathway genes, and cholesterol pathway genes. However,**
89 **we had not reported associations between SREBF and Notch pathway and cholesterol**

90 pathway genes. We have thus analysed this relationship by O-PLS modelling and
91 similar to *APOA1BP* we have found significant models between *SREBF1* and Notch
92 and cholesterol genes, respectively. We have added these results in the revised version
93 of the manuscript. Therefore, lower *APOA1BP* expression is associated with higher
94 expression of *SREBF1* and *NOTCH* receptors, which in turn are associated with
95 higher levels of blood cells and atherosclerosis measures. We have also found
96 significant associations between several white blood cells and atherosclerosis
97 measures. Although we had not reported these associations in the original
98 manuscript, we have added them in supplementary Figure 1d. Thus, we found a clear
99 association among the *APOA1BP-SREBF-NOTCH* axis, haematopoiesis and
100 atherosclerosis.

101

102 2. Please explain the difference in the correlation between gene expression (e.g.,
103 *APOA1BP*, *SREBF*, and *NOTCH*) and parameters for atherosclerosis in left/right carotid
104 arteries (Page13).

105 *APOA1BP* was negatively associated with measurements in both left and right
106 carotid arteries. Interestingly, *SREBF1* was mainly positively associated with all the
107 measurements in the left carotid artery, which would be in agreement with recent
108 evidence that the left carotid artery is more vulnerable to atherosclerosis than the
109 right carotid artery [1,2]. This is also consistent with *NOTCH1* and *NOTCH4*
110 positively associated with atherosclerosis measures in the left carotid artery. We have
111 added this information in the discussion. In the case of *NOTCH2NL* though, it
112 correlated with measures of the right internal carotid artery, but the reason for this
113 association would need further investigations.

114 [1] Selwaness M, Van Den Bouwhuijsen Q, Van Onkelen RS, Hofman A, Franco OH,
115 Van Der Lugt A, et al. Atherosclerotic plaque in the left carotid artery is more
116 vulnerable than in the right. *Stroke* 2014;45:3226–30.
117 doi:10.1161/STROKEAHA.114.005202.

118 [2] Chou CL, Wu YJ, Hung CL, Liu CC, Wang S De, Wu TW, et al. Segment-specific
119 prevalence of carotid artery plaque and stenosis in middle-aged adults and elders in

120 Taiwan: A community-based study. J Formos Med Assoc 2019;118:64–71.
121 doi:10.1016/j.jfma.2018.01.009.

122

123 3. *How do "APOA1BP", "SREBF", and "NOTCH" interact each other?*

124 **From O-PLS modelling and further validation by partial Spearman correlation**
125 **(adjusting for age, BMI, sex, and country) we had found significant associations**
126 **between the expression of APOA1BP and NOTCH pathway genes. We also showed**
127 **that APOA1BP and SREBF1 had opposite associations with the almost the same**
128 **atherosclerosis measures, particularly mLCCA, mCCA, and mCA. However, we had**
129 **not shown a direct relationship between SREBF and NOTCH. Thus, similar to what**
130 **we did for the associations between APOA1BP expression and Notch and cholesterol**
131 **pathway associated genes, we built O-PLS models between the expression of SREBF1**
132 **and Notch and cholesterol genes, respectively. In both cases, we obtained significant**
133 **models ($P<0.001$) associating SREBF1 with Notch and cholesterol pathways. Both**
134 **models were further validated by partial Spearman's correlation. Interestingly, the**
135 **expression of SREBF1 was positively associated with both NOTCH1 and ABCA1**
136 **expression, which we had found negatively associated with APOA1BP. In the case of**
137 **SREBF2, however, we did not find significant associations with the Notch pathway**
138 **genes. We have added all these results in the results section and we have created a**
139 **new Supplementary Figure 2. Therefore, we have found a clear relationship between**
140 **APOA1BP, SREBF, and NOTCH, but due to the cross-sectional nature of our study**
141 **we cannot infer causal mechanisms or the direction of the associations.**

142

143 4. *The authors only described about Jagged ligand related with Notch. A previous study*
144 *demonstrated the inhibition of Dll4, a Notch ligand, reduced lipid accumulation in the*
145 *liver (PNAS 2012;109:E1868-E1877.).*

146 **Thanks for pointing this. In Figure 11 we only showed the significant associations that**
147 **we obtained between APOA1BP and genes from the Notch pathway. However, the O-**
148 **PLS models were performed considering 79 genes involved in the Notch signalling**
149 **pathway. Then, significant genes identified through O-PLS modeling were further**

150 validated by partial Spearman's correlation. These 79 genes included both jagged
151 and delta-like ligands, but we did not find significant associations between delta-like
152 ligand and *APOA1BP* expression. We only found significant associations with jagged
153 ligands. Because of this, we have not discussed delta-like ligands in the manuscript.
154 To avoid confusions, we have added the number of genes that we considered to build
155 the O-PLS models based on Notch signalling pathway associated genes and
156 cholesterol pathway associated genes in the revised version of the manuscript. We
157 have also added the names of these genes in the Supplementary Tables 1 and 2,
158 respectively.

159

160 On the other hand, in our liver samples, only *DLL1*, *DLK1* (delta like non-canonical
161 Notch ligand1), and *DLK2* were expressed, but not *DLL4*. Considering Fukuda *et al.*
162 results suggested by the reviewer, we have analysed the possible association between
163 delta-like ligands and steatosis. Thus, we have performed partial Spearman's
164 correlation analysis between these delta ligands and the steatosis degree in our
165 population. However, we have not found any significant association, although the
166 expression of *DLK1* had a trend towards a positive association with the degree of
167 steatosis ($r=0.21$, $p=0.076$). We must also take into account that Fukuda *et al.* treated
168 mice with anti-mouse *Dll4* antibody, which inhibits *Dll4* in all *Dll4*-expressing cells,
169 not just the liver. Therefore, decreases in the accumulation of lipids in the liver after
170 *Dll4* Ab treatment could originate from blockage of *Dll4* in other tissues. In fact, *Dll4*
171 Ab treatment also reduced fat in epididymal and sub-cutaneous adipose tissues.

172

173 *5. Do the authors have data associated with inflammation directly?*

174 From multivariate analyses, we have found direct associations of *SREBF1* and
175 *SREBF2* expression with *N*-acetylglycoproteins (NAG) measured by NMR. It is a
176 composite biomarker of systemic inflammation that integrates the protein levels and
177 glycosylation states of several of the most abundant acute phase proteins in serum. As
178 a composite biomarker, NAG is a novel marker of systemic inflammation that may be
179 a better reflection of systemic acute phase response than any other single

180 glycoprotein component. For example, it has low intra-individual variability
181 compared to hsCRP, which often exhibits high intra-individual variability, allowing a
182 more stable measure of inflammation.

183

184 We have now specifically analysed the correlation between NAG and *APOA1BP* and
185 *NOTCH* receptors. We have found an almost significant association between NAG
186 and *APOA1BP* ($r=-0.22$, $p=0.051$). We have also found a trend towards a positive
187 association between *NOTCH2NL* and NAG ($r=0.20$, $p=0.07$), but no significant
188 associations with the expression of the other Notch receptors. We have added these
189 results in the results section.

190

191 We have also realized that although in lines 491-493 we had commented that NAG
192 was associated with cIMT measures, we had not reported the associations in the
193 results section. Therefore, we have added a heatmap in Supplementary Figure 1b
194 with the correlations between NAG and measures of atherosclerosis. As expected,
195 several of these measures correlated positively with NAG.

196

197 *6. Can the authors show the correlation between gene expression (e.g., APOA1BP,*
198 *SREBF, and NOTCH) and WBC population such as monocyte or lymphocytes?*

199 We have added a heatmap in Supplementary Figure 1c with the correlations of
200 haematological parameters (total WBC, lymphocytes, monocytes, eosinophils,
201 neutrophils, red blood cells, and platelets) with the expression *APOA1BP*, *SREBF*
202 and *NOTCH* genes.

203

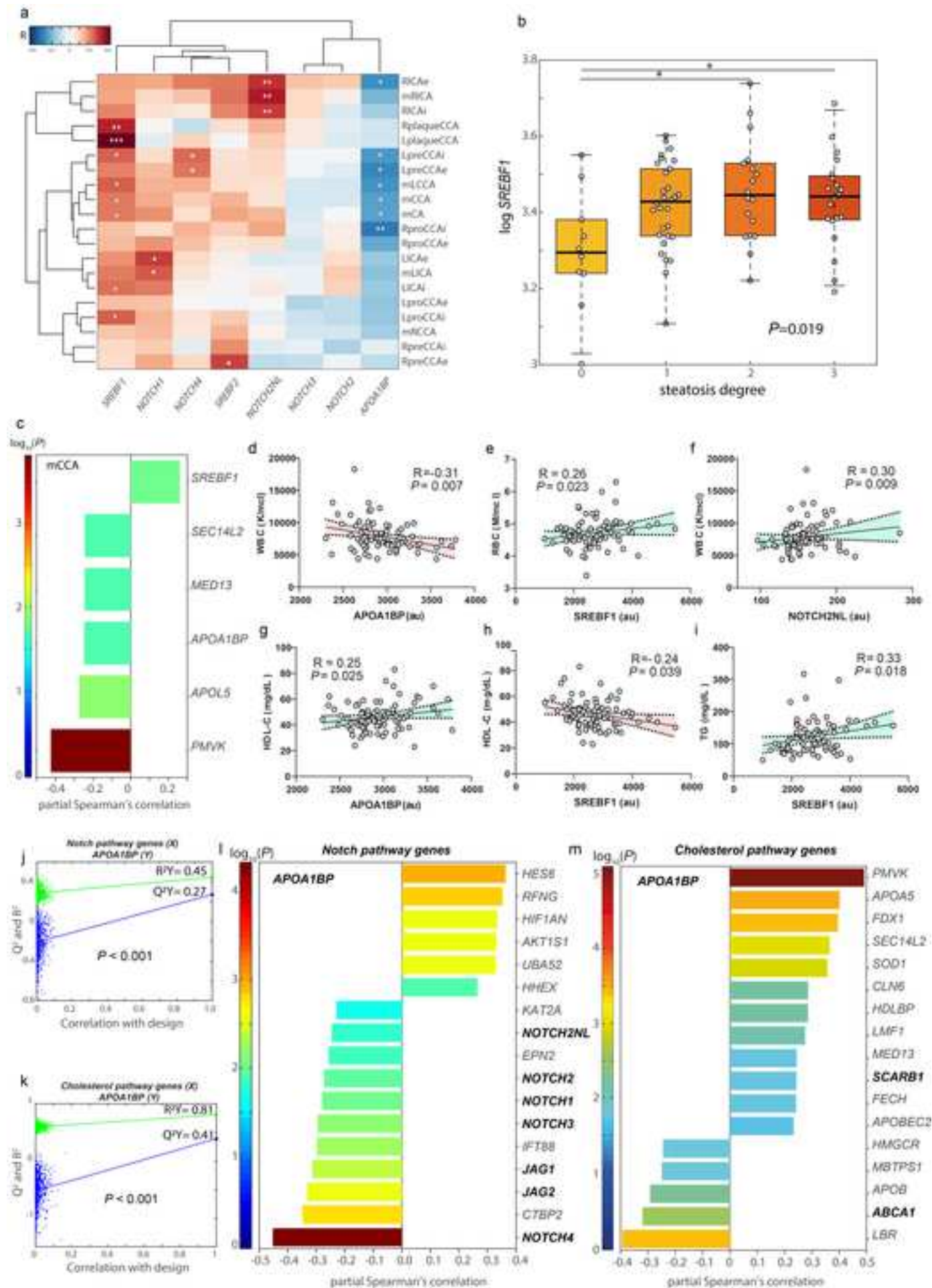
204 *7. Can the author apply the results of present study to general population? If not, the*
205 *authors need to make this clear in the title of this paper.*

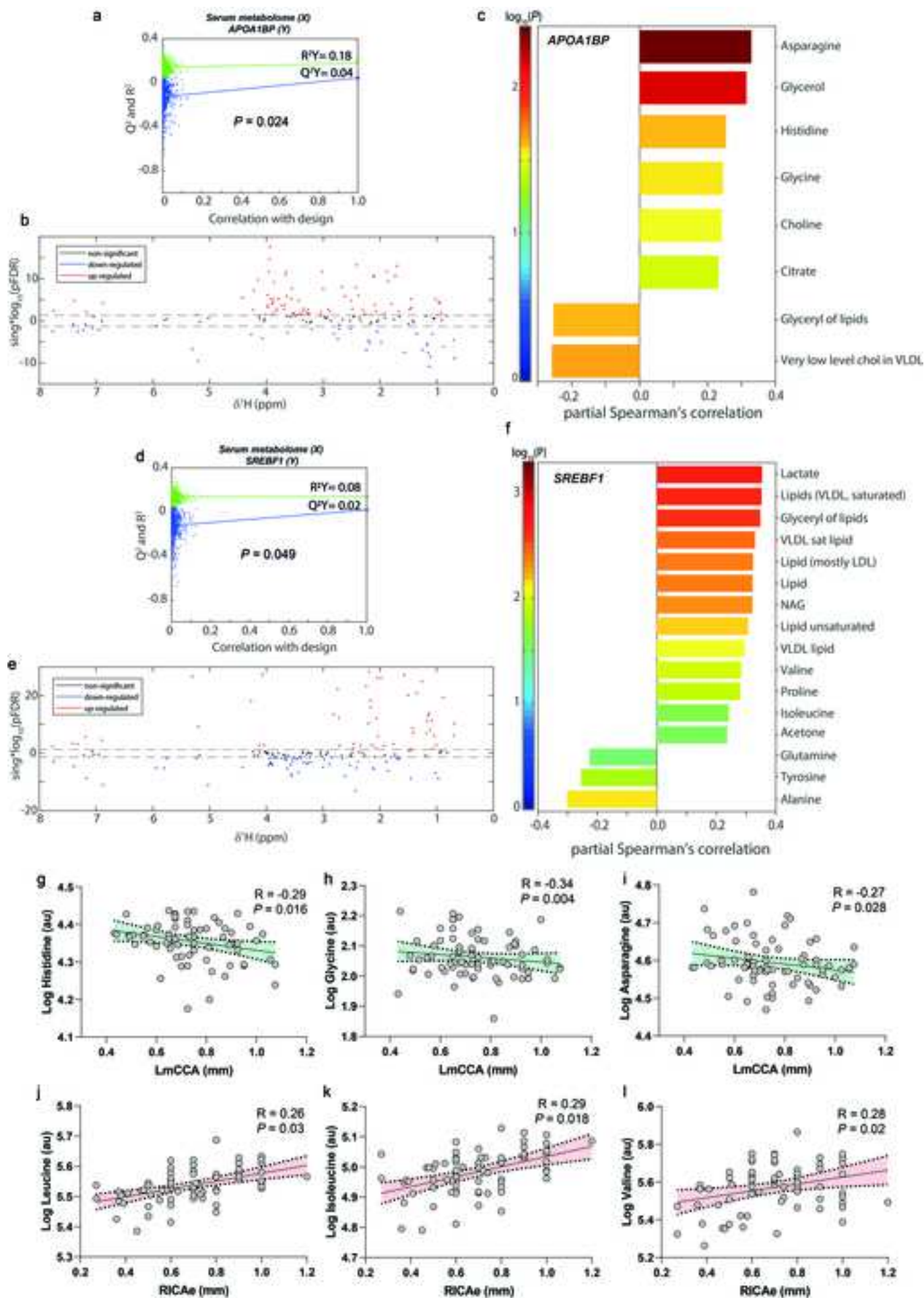
206 As our population consisted in morbidly obese patients, the results may not be
207 generalizable to the general population. Following the reviewer's suggestion we have
208 modified the title and now it reads as: "The *APOA1BP-SREBF-NOTCH* axis is
209 associated with reduced atherosclerosis risk in morbidly obese patients".

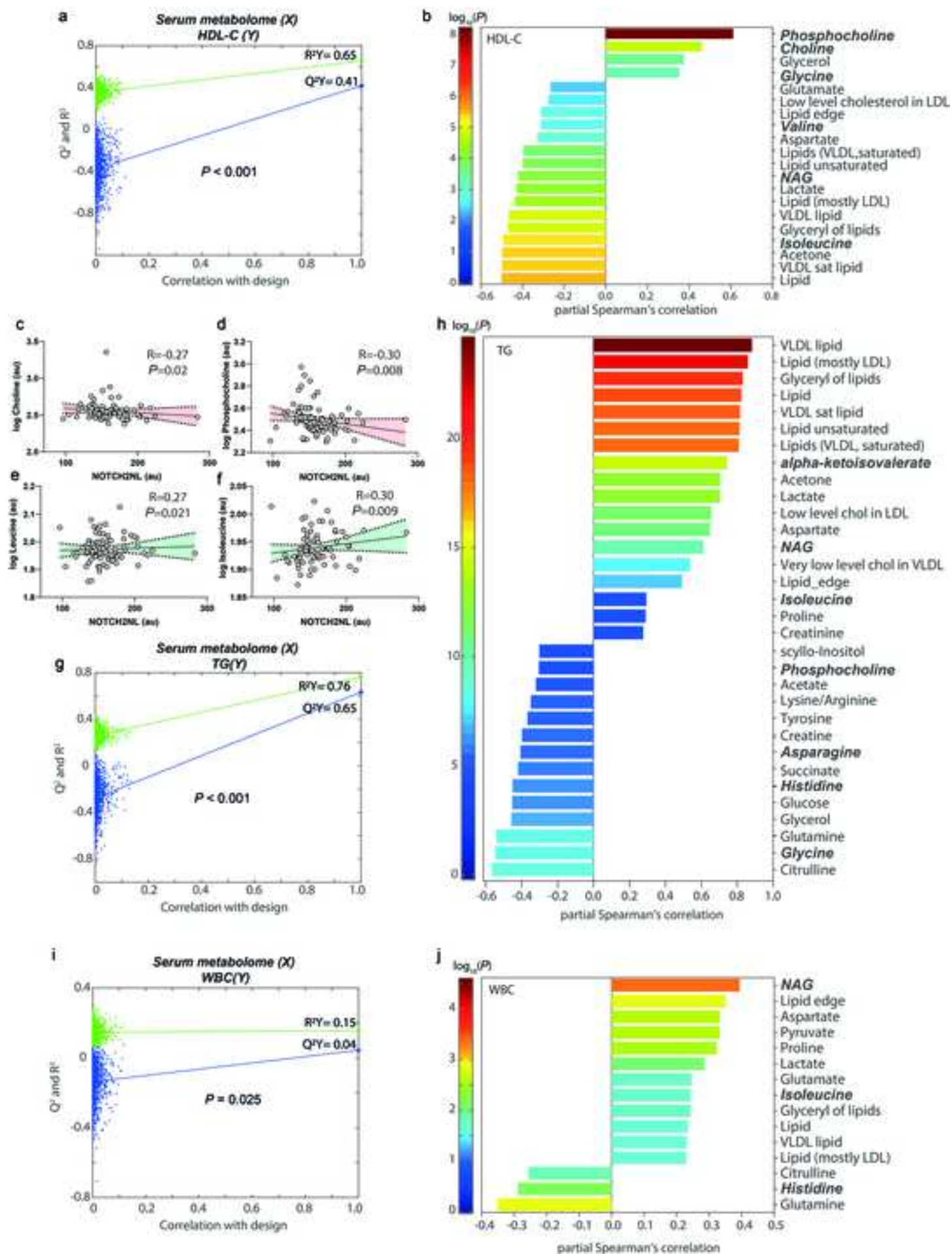
210 **Comments to the Editor**

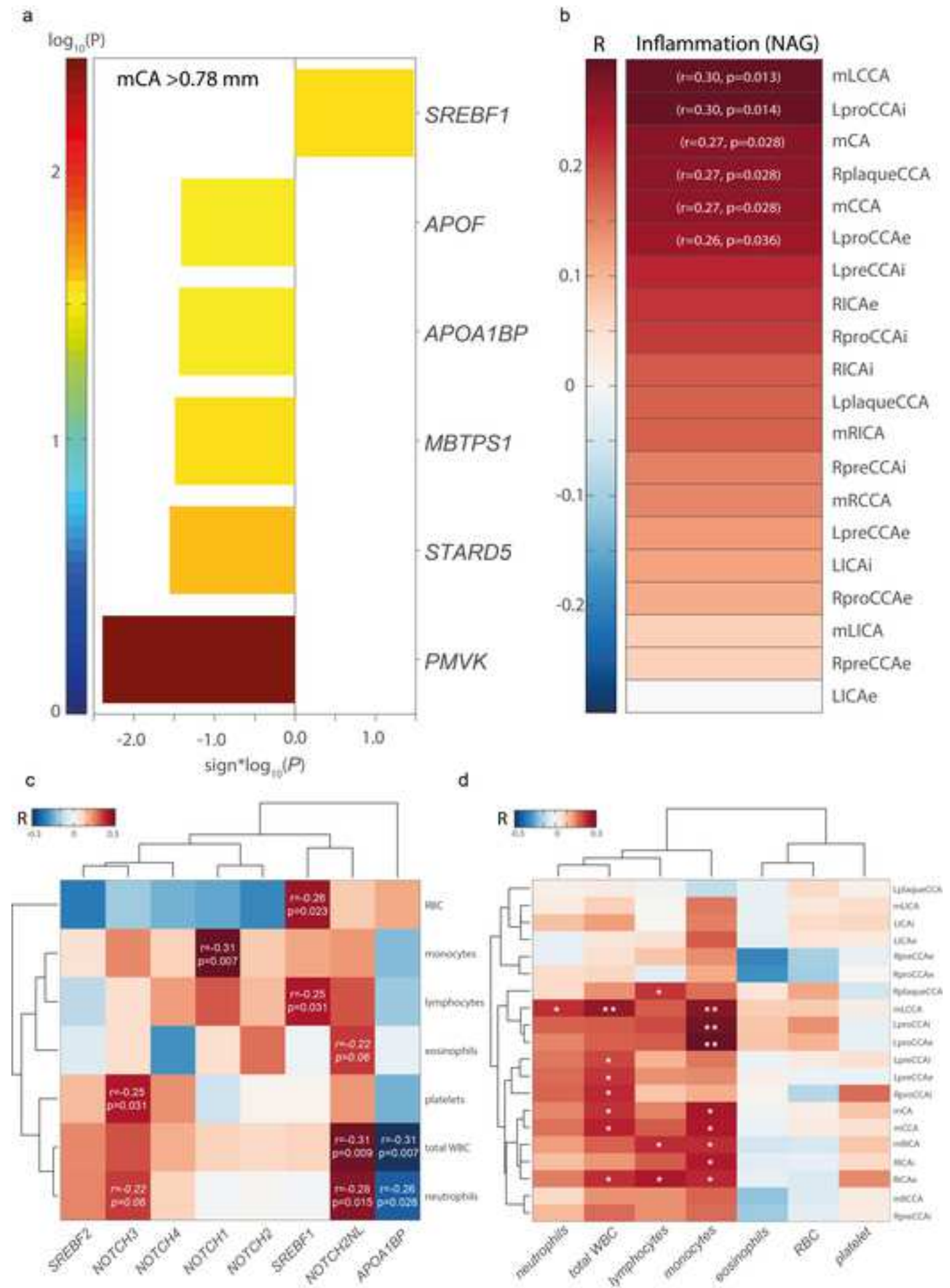
211

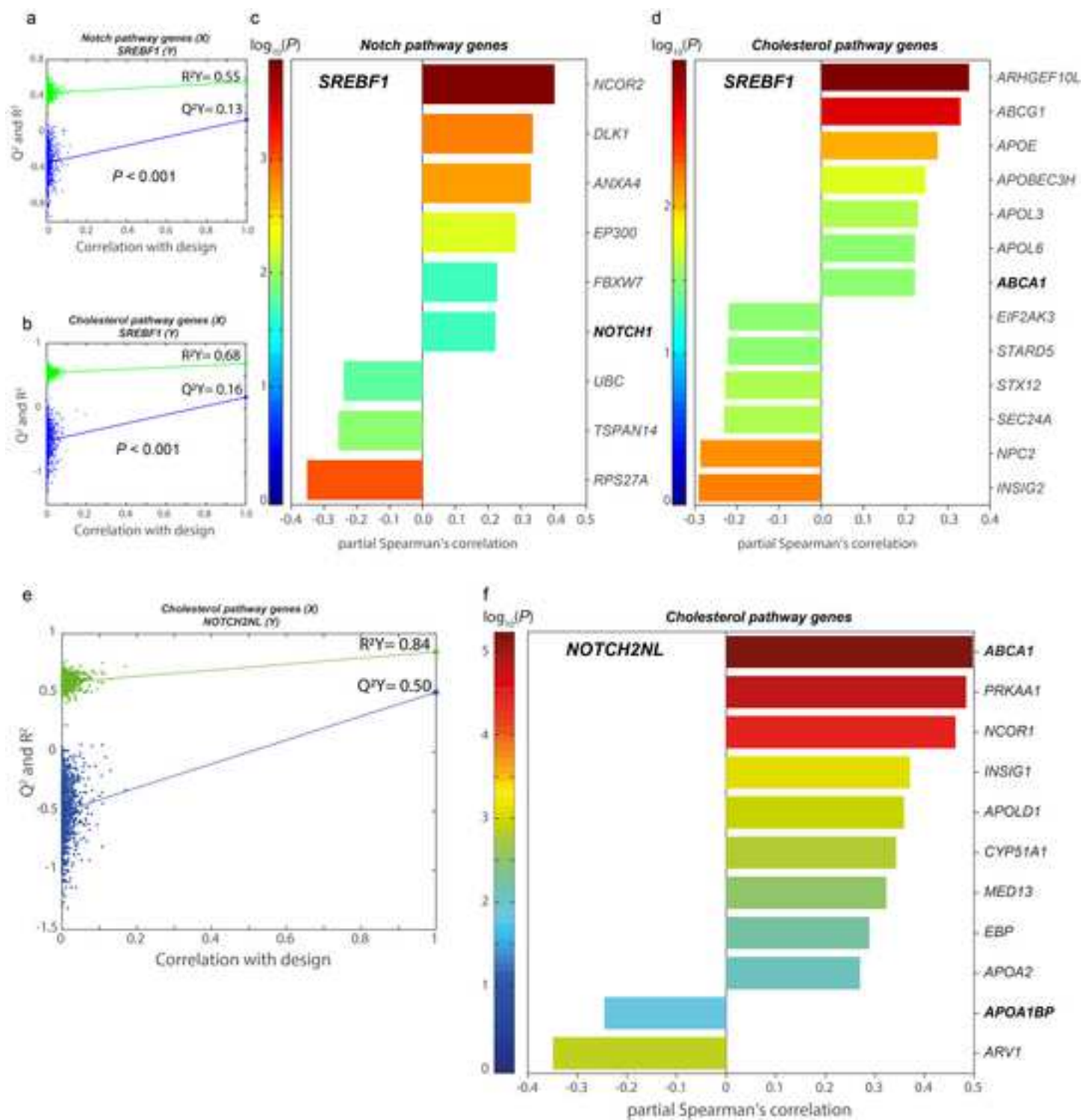
212 **We have added Dr. Josep Puig as an author in the paper. He was the person**
213 **responsible for the measurements of carotid intima-media thickness, but as he has**
214 **moved to another area we had forgotten to add him as an author. We apologise for**
215 **this mistake and any inconvenience it may have caused.**

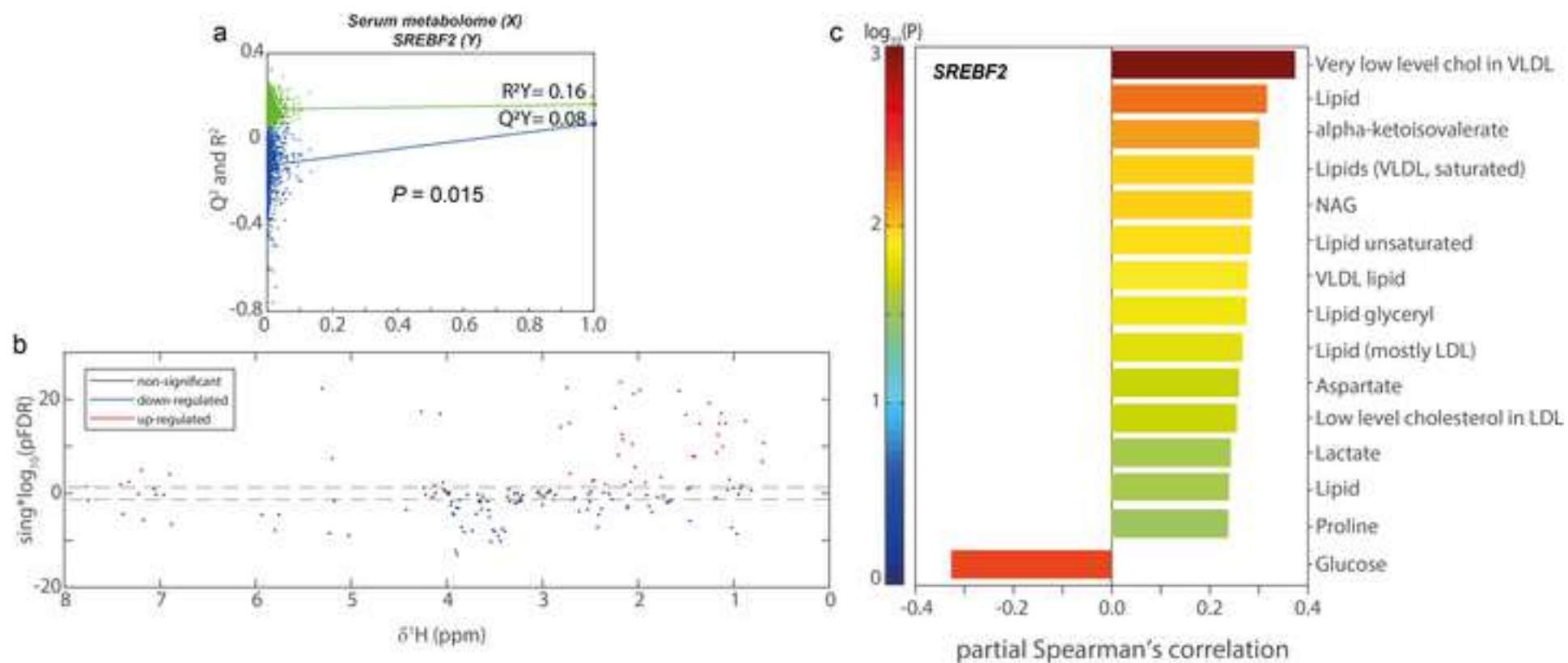












Supplementary Table 1. Notch signalling pathway associated genes considered in the present study.

Genes
<i>AAK1</i>
<i>ADAM10</i>
<i>AKT1S1</i>
<i>ANXA4</i>
<i>APP</i>
<i>BMP2</i>
<i>CBFA2T2</i>
<i>CDK6</i>
<i>CDKN1B</i>
<i>CIR1</i>
<i>CREB1</i>
<i>CREBBP</i>
<i>CTBP1</i>
<i>CTBP2</i>
<i>DLK1</i>
<i>DLL1</i>
<i>DVL1</i>
<i>DVL3</i>
<i>EP300</i>
<i>EPN1</i>
<i>EPN2</i>
<i>FBXW7</i>
<i>FOXC1</i>
<i>GALNT11</i>
<i>GMDS</i>
<i>GOT1</i>
<i>HDAC1</i>
<i>HDAC2</i>
<i>HES1</i>
<i>HES2</i>
<i>HES4</i>
<i>HES5</i>
<i>HES6</i>
<i>HES7</i>
<i>HESX1</i>
<i>HEY1</i>
<i>HEY2</i>
<i>HHEX</i>
<i>HIF1AN</i>
<i>IFT172</i>
<i>IFT88</i>

<i>JAG1</i>
<i>JAG2</i>
<i>KAT2A</i>
<i>KAT2B</i>
<i>MAML1</i>
<i>MAML2</i>
<i>MIB1</i>
<i>MIB2</i>
<i>MMP14</i>
<i>NCOR2</i>
<i>NCSTN</i>
<i>NEURL</i>
<i>NFKBIA</i>
<i>NLE1</i>
<i>NOTCH1</i>
<i>NOTCH2</i>
<i>NOTCH2NL</i>
<i>NOTCH3</i>
<i>NOTCH4</i>
<i>POFUT1</i>
<i>POGLUT1</i>
<i>PSEN2</i>
<i>PTP4A3</i>
<i>RBM15</i>
<i>RBPJ</i>
<i>RFNG</i>
<i>RPS19</i>
<i>RPS27A</i>
<i>SEL1L</i>
<i>SNAI2</i>
<i>SORBS2</i>
<i>SPEN</i>
<i>TSPAN14</i>
<i>TSPAN15</i>
<i>UBA52</i>
<i>UBB</i>
<i>UBC</i>
<i>WDR12</i>

Supplementary Table 2. Notch signalling pathway associated genes considered in the present study.

Genes
<i>ABCA1</i>
<i>ABCG1</i>
<i>ACADL</i>
<i>ACAT2</i>
<i>ALMS1</i>
<i>APLP2</i>
<i>APOA1</i>
<i>APOA1BP</i>
<i>APOA2</i>
<i>APOA4</i>
<i>APOA5</i>
<i>APOB</i>
<i>APOBEC2</i>
<i>APOBEC3A</i>
<i>APOBEC3B</i>
<i>APOBEC3C</i>
<i>APOBEC3D</i>
<i>APOBEC3F</i>
<i>APOBEC3G</i>
<i>APOBEC3H</i>
<i>APOBR</i>
<i>APOC1</i>
<i>APOC2</i>
<i>APOC3</i>
<i>APOC4</i>
<i>APOE</i>
<i>APOF</i>
<i>APOH</i>
<i>APOL1</i>
<i>APOL2</i>
<i>APOL3</i>
<i>APOL4</i>
<i>APOL5</i>
<i>APOL6</i>
<i>APOLD1</i>
<i>ARHGEF10L</i>
<i>ARV1</i>
<i>CAT</i>
<i>CLN6</i>
<i>CYB5R1</i>
<i>CYB5R3</i>

<i>CYP51A1</i>
<i>DHCR24</i>
<i>DHCR7</i>
<i>EBP</i>
<i>EBPL</i>
<i>EHD1</i>
<i>EIF2A</i>
<i>EIF2AK3</i>
<i>ERLIN1</i>
<i>ERLIN2</i>
<i>FDFT1</i>
<i>FDPS</i>
<i>FDX1</i>
<i>FECH</i>
<i>HDLBP</i>
<i>HMGCR</i>
<i>HSD17B7</i>
<i>INSIG1</i>
<i>INSIG2</i>
<i>IRAK1</i>
<i>LBR</i>
<i>LDLR</i>
<i>LDLRAP1</i>
<i>LIPA</i>
<i>LIPE</i>
<i>LMF1</i>
<i>LMNA</i>
<i>LRP5</i>
<i>LRP6</i>
<i>LSS</i>
<i>MBTPS1</i>
<i>MED13</i>
<i>MVD</i>
<i>MVK</i>
<i>NCOR1</i>
<i>NPC1</i>
<i>NPC1L1</i>
<i>NPC2</i>
<i>NR1H2</i>
<i>NR1H3</i>
<i>NUS1</i>
<i>OSBP</i>
<i>PCTP</i>
<i>PLSCR3</i>
<i>PMVK</i>

<i>POR</i>
<i>PRKAA1</i>
<i>PTCH1</i>
<i>RALY</i>
<i>RORA</i>
<i>SC5DL</i>
<i>SCAP</i>
<i>SCARB1</i>
<i>SCP2</i>
<i>SEC14L2</i>
<i>SEC24A</i>
<i>SIRT1</i>
<i>SOD1</i>
<i>SQLE</i>
<i>SREBF1</i>
<i>SREBF2</i>
<i>STARD4</i>
<i>STARD5</i>
<i>STX12</i>
<i>TM7SF2</i>
<i>TMEM97</i>
<i>VPS4A</i>
<i>XBP1</i>